



Comparative neuroanatomy of ctenophores: Neural and muscular systems in *Euplokamis dunlapae* and related species

Tigran P. Norekian^{1,2,3,4} | Leonid L. Moroz^{1,5}

¹Whitney Laboratory for Marine Bioscience, University of Florida, St. Augustine, Florida

²Friday Harbor Laboratories, University of Washington, Friday Harbor, Washington

³Institute of Higher Nervous Activity and Neurophysiology, Russian Academy of Sciences, Moscow, Russia

⁴The Kovalevsky Institute of Marine Biological Research, Russian Academy of Sciences, Moscow, Russia

⁵Department of Neuroscience and McKnight Brain Institute, University of Florida, Gainesville, Florida

Correspondence

Leonid L. Moroz, Department of Neuroscience and The Whitney Laboratory, University of Florida, 9505 Ocean Shore Blvd. St. Augustine, FL 32080.

Email: moroz@whitney.ufl.edu

Funding information

Directorate for Biological Sciences, Grant/Award Numbers: 1146575, 1557923, 1645219; Ministry of Education and Science of the Russian Federation, Grant/Award Number: 14.W03.31.0015; National Science Foundation, Grant/Award Number: 1548121; National Aeronautics and Space Administration, Grant/Award Number: NASA-NNX13AJ31G

Peer Review

The peer review history for this article is available at <https://publons.com/publon/10.1002/cne.24770>.

Abstract

Ctenophora is an early-branching basal metazoan lineage, which may have evolved neurons and muscles independently from other animals. However, despite the profound diversity among ctenophores, basal neuroanatomical data are limited to representatives of two genera. Here, we describe the organization of neuromuscular systems in eight ctenophore species focusing on *Euplokamis dunlapae*—the representative of the lineage sister to all other ctenophores. Cydippids (*Hormiphora hormiphora* and *Dryodora glandiformis*) and lobates (*Bolinopsis infundibulum* and *Mnemiopsis leidyi*) were used as reference platforms to cover both morphological and ecological diversity within the phylum. We show that even with substantial environmental differences, the basal organization of neural systems is conserved among ctenophores. In all species, we detected two distributed neuronal subsystems: the subepithelial polygonal network and the mesogleal elements. Nevertheless, each species developed specific innovations in neural, muscular, and receptor systems. Most notable *Euplokamis*-specific features are the following: (a) Comb nerves with giant axons. These nerves directly coordinate the rapid escape response bypassing the central integrative structure known as the aboral sensory organ. (b) Neural processes in tentacles along the rows of “boxes” providing structural support and located under striated muscles. (c) Radial muscles that cross the mesoglea and connect the outer wall to the aboral canal. (d) Flat muscles, encircling each meridional canal. Also, we detected a structurally different rectangular neural network in the feeding lobes of Lobata (*Mnemiopsis/Bolinopsis*) but not in other species. The described lineage-specific innovations can be used for future single-cell atlases of ctenophores and analyses of neuronal evolution in basal metazoans.

KEY WORDS

apical organ, *Beroe*, cell atlas, cilia, Ctenophora, development, evolution, F-actin, mesoglea, microvilli, *Mnemiopsis*, muscle system, nervous system, phylogeny, *Pleurobrachia*, receptors, sensory cells, Stereocilia, tubulin

1 | INTRODUCTION

Ctenophores or comb jellies are one of the early-branching basal metazoan lineages comprising about 200 marine species with highly

diverse morphology, body plans, ecological and behavior adaptations (Brusca & Brusca, 2003; Dunlap, 1974; Hernandez-Nicaise, 1991; Kozloff, 1990; Tamm, 1982; Tamm, 2014). Most recent genomic and phylogenomic data indicate that Ctenophora is the sister group to the rest of animals (Arcila et al., 2017; Borowiec, Lee, Chiu, & Plachetzki, 2015; Moroz et al., 2014; Shen, Hittinger, & Rokas, 2017; Whelan et al., 2017; Whelan, Kocot, Moroz, & Halanych, 2015), although such position is a subject of hot debates over the last years (Dunn, 2017; Dunn et al., 2008; Halanych, 2015; Simion et al., 2017; Telford, Moroz, & Halanych, 2016). Irrespective of the precise phylogenomic placement of this enigmatic group, genomic and molecular data strongly suggest that ctenophores evolved neural and muscular systems as well as mesoderm and sensory structures independently from the rest of animals (Moroz, 2014; Moroz, 2015; Moroz et al., 2014; Moroz & Kohn, 2015, 2016). However, even basal neuroanatomical data are limited to representatives of just two genera—the sea gooseberry *Pleurobrachia* (Jager et al., 2011; Jager et al., 2013; Norekian & Moroz, 2016, 2019b) and the lobate *Beroe* (Norekian & Moroz, 2019a).

Here, we describe the organization of neuromuscular systems in representatives of eight ctenophore species focusing on the cydippid *E. dunlapae* (Granhag, Majaneva, & Møller, 2012; Mills, 1987). The selection of this species as the major model for this study is based on two key factors. First, phylogenomic analyses placed the *Euplokamis* lineage as the sister to the rest of the ctenophores sequenced so far (Moroz et al., 2014; Whelan et al., 2017). Second, *Euplokamis* has a very complex behavior including a rapid startle response, which is supported by the system of giant axons and striated muscles in the tentacles (Chun, 1880; Mackie, Mills, & Singla, 1988; Mackie, Mills, & Singla, 1992; Mills, 1987). Each of these adaptations represents a unique example of convergent evolution within integrative and locomotor systems (Moroz et al., 2014; Whelan et al., 2017). It appears that striated muscles evolved at least three times independently in animals (Steinmetz et al., 2012); and giant axons in *Euplokamis* might be analogous to those in squids but implicated in the control of ciliated structures (Mackie et al., 1992).

In contrast to *Euplokamis*, other species from this study are representatives of quite derived ctenophore lineages (Dunn, 2017; Dunn, Leys, & Haddock, 2015; Johansson et al., 2018; Moroz et al., 2014; Whelan et al., 2017). Recent phylogenomic reconstructions, using transcriptomes of 37 ctenophore species, proposed that about 380–260 million years ago Ctenophora might undergo a substantial evolutionary bottleneck (Whelan et al., 2017) with the extinction of several early groups followed by adaptive radiation leading to extant lineages. Due to distinct feeding adaptations, the lineages leading to *Bolinopsis* lost some ancestral traits such as tentacles in adult stages, whereas *Beroe* lost tentacles permanently (Tamm, 1982; Tamm, 2014).

Our study shows that despite substantial ecological differences, the basal organization of neural systems is conserved among ctenophores, consistent with earlier morphological observations using methylene blue vital staining and silver impregnation (Hernandez-Nicaise, 1991). In all species, we detected two distributed neuronal

subsystems: the subepithelial polygonal network and the mesogleal elements. However, we identified several species-specific innovations in both muscular and receptor systems, reflecting their ecological and behavioral differences. The present work might also serve as a reference platform for future single-cell atlases of ctenophores and analyses of neuronal evolution (Moroz, 2018; Sebe-Pedros et al., 2018; Striedter et al., 2014).

2 | MATERIALS AND METHODS

2.1 | Animals

Adult *E. dunlapae* (Mills, 1987) were collected from the breakwater and held in 1-gal glass jars in the large tanks with constantly circulating seawater at 10–12°C. Experiments were carried out at Friday Harbor Laboratories, the University of Washington in the spring–summer seasons of 2011–2019. Most *Euplokamis* (about 30) were collected in the unusually plentiful for such deep-water species season of the year 2012.

Other ctenophore species such as *D. glandiformis*, *B. infundibulum*, and *H. hormiphora* were also collected at Friday Harbor Laboratories. *M. leidyi* was obtained from Woods Hole Marine Biological Laboratory. We also collected *Beroe ovata*, *M. leidyi*, and *Pleurobrachia pileus* from the Black Sea. Also, at Friday Harbor Laboratories, we obtained a novel *Mertensiidae* species (Dr. C. Mills, unpublished), which belongs to highly derived cydippids, as described in recent phylogenomic papers (Moroz et al., 2014; Whelan et al., 2017).

2.2 | Immunocytochemistry and Phalloidin staining

Adult animals were fixed overnight in 4% paraformaldehyde in 0.1 M phosphate-buffered saline (PBS) at +5°C and washed for 2 hr in PBS. Ctenophores from the Lobata order (*Bolinopsis* and *Mnemiopsis*) due to their highly fragile gelatinous texture almost completely disintegrated during the fixation process and, therefore, were not very reliable for immunohistochemical studies. We could only partially preserve their tissues for labeling with the outcome of less than 5% in regular fixative. Therefore, a new fixation procedure was developed for these species, which was much more successful in preserving the tissue. We used 1:1 mixture of 6% paraformaldehyde in filtered seawater and 100% ethanol, plus 0.5% acetic acid at –20°C for 1 hr and then at +5°C for 12 hr or overnight.

The fixed animals were dissected and pre-incubated overnight in a blocking solution of 6% goat serum in PBS. The tissues were then incubated for 48 hr at +5°C in the primary antibodies diluted in 6% of the goat serum at a final dilution 1:40. We used the rat monoclonal antibody (AbD Serotec Cat# MCA77G, RRID: AB_325003), which recognizes the alpha subunit of tubulin and specifically binds tyrosylated tubulin (Wehland & Willingham, 1983; Wehland, Willingham, & Sandoval, 1983). Following a series of PBS washes for total 6 hr, the tissues were incubated for 12 hr in secondary goat anti-rat IgG antibodies: Alexa Fluor 488 conjugated (Molecular Probes, Invitrogen, Cat# A11006, RRID: AB_141373) or Alexa Fluor 568 conjugated

(Molecular Probes, Invitrogen, Cat# A11077, RRID: AB_2534121), at a final dilution 1:20.

To label the muscle fibers, we used well-known marker phalloidin (Alexa Fluor 488 and Alexa Fluor 568 phalloidins from Molecular Probes), which binds to F-actin (Wulf, Deboden, Bautz, Faulstich, & Wieland, 1979). After washing in PBS following the secondary antibody treatment, the tissue was incubated in phalloidin solution (in PBS) for 4 to 8 hr at a final dilution 1:80 and then washed in several PBS rinses for 6 hr.

The preparations were mounted in Fluorescent Mounting Media (KPL) on glass microscope slides to be viewed using a Nikon Research Microscope Eclipse E800 with Epi-fluorescence using standard TRITC and FITC filters and recorded using BioRad (Radiance 2000) and Nikon C2 Laser Scanning confocal microscope. To stain nuclei, the tissues were mounted in VECTASHIELD Hard-Set Mounting Medium with DAPI (Cat# H-1500). To test for the specificity of immunostaining, either the primary or the secondary antibody were omitted from the procedure. In both cases, no labeling was detected. The rat monoclonal anti-tyrosylated alpha-tubulin antibody has also been used in two different species of *Pleurobrachia* and *Beroe abyssicola* (Jager et al., 2011; Jager et al., 2013; Moroz, 2015; Norekian & Moroz, 2016, 2019a, 2019b).

2.3 | Antibody specificity

Rat monoclonal anti-tyrosylated alpha-tubulin antibody is raised against yeast tubulin, clone YL1/2, isotype IgG2a (Serotec Cat # MCA77G; RRID: AB_325003). The antibody is routinely tested in ELISA on tubulin, and the close-related ctenophore *Pleurobrachia* is

listed in species reactivity (manufacturer's technical information). The epitope recognized by this antibody appears to be a linear sequence requiring an aromatic residue at the C terminus, with the two adjacent amino acids being negatively charged, represented by Glu-Glu-Tyr in Tyr-Tubulin (manufacturer's information). As reported by Wehland et al. (Wehland et al., 1983; Wehland & Willingham, 1983), this rat monoclonal antibody "reacts specifically with the tyrosylated form of brain alpha-tubulin from different species." They showed that "YL 1/2 reacts with the synthetic peptide Gly-(Glu)3-Gly-(Glu)2-Tyr, corresponding to the carboxyterminal amino acid sequence of tyrosylated alpha-tubulin but does not react with Gly-(Glu)3-Gly-(Glu)2, the constituent peptide of detyrosinated alpha-tubulin." The epitope recognized by this antibody has been extensively studied, including details about antibody specificity and relevant assays (Wehland et al., 1983; Wehland & Willingham, 1983). Equally important, this specific monoclonal antibody has been used before in three different species of both adult and larval *Pleurobrachia* and *Beroe*, the previously obtained staining patterns were very similar to already published experiments (Jager et al., 2011; Jager et al., 2013; Moroz, 2015; Norekian & Moroz, 2016, 2019a, 2019b).

3 | RESULTS

In this study, we primarily focused on *E. dunlapae* and used other ctenophores as reference species for initial comparative neuroanatomy screening. Most of the other species were either significantly less abundant (e.g., *D. glandiformis*, *H. hormiphora*, and *Mertensiidae* species) with only a few individuals available over the several years of

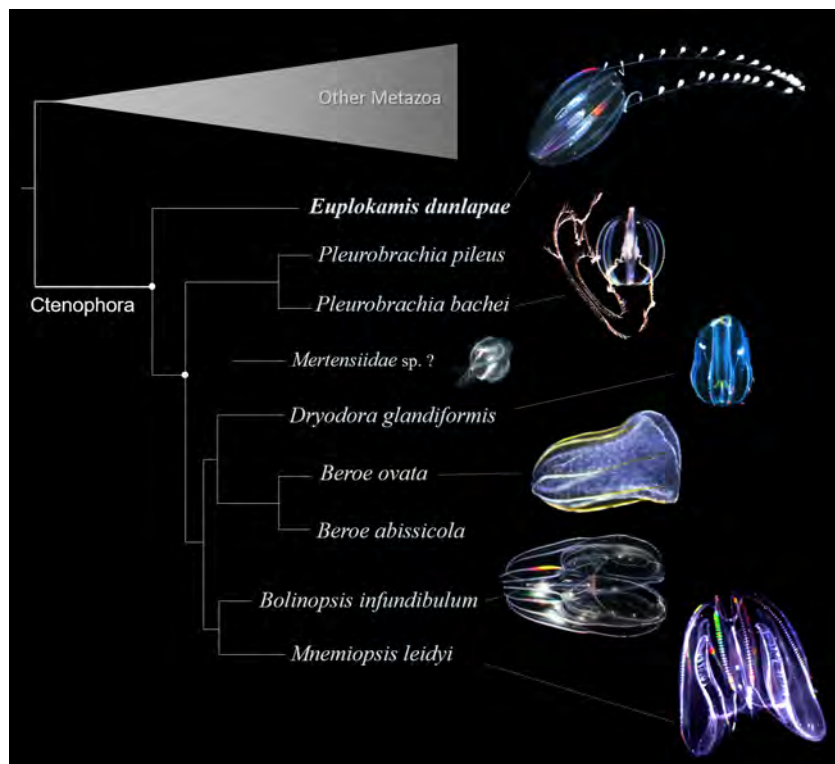


FIGURE 1 The relationships among comb jellies, used in this study, with a position of *Euplokamis* as a representative of the sister lineage to the rest of Ctenophora (modified from Moroz et al., 2014 and Whelan et al., 2017) [Color figure can be viewed at wileyonlinelibrary.com]

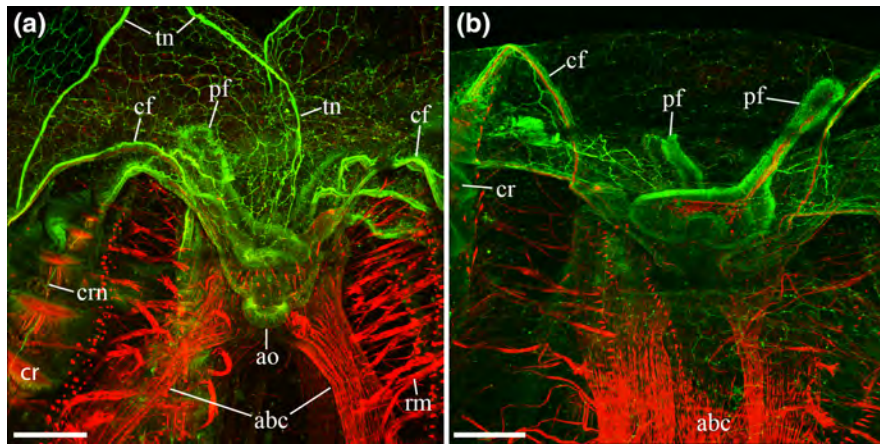


FIGURE 2 The aboral organ complex in *Euplokamis* as revealed by the tubulin antibody (green) and phalloidin/F-actin labeling (red). a, Neuronal elements in a partially retracted aboral organ (*ao*) and polar fields (*pf*). Note that the entire body wall surface is covered by a polygonal neural network with tubulin IR neurons and their processes (green). Both tentacle nerves (*tn*) and comb row nerve (*crn*) are visible. Thin walls of the aboral canal with muscle filaments stained by phalloidin were naturally pulled apart in this preparation, presumably by radial muscles. b, Polar fields are not retracted and shown in their normal “relaxed” state. *abc*, aboral canal; *cf*, ciliated furrow; *cr*, comb row; *rm*, radial muscles. Scale bars: a, b: 200 μ m [Color figure can be viewed at wileyonlinelibrary.com]

collections, or more abundant species, such as *Bolinopsis* and *Mnemiopsis*, were extremely fragile (Figure 1).

3.1 | Introduction to the species

The general anatomy and behaviors of *E. dunlapae* have been described in detail by Claudia Mills and George O. Mackie (Mackie et al., 1992; Mills, 1987). Although *Euplokamis* has a typical cydippid body plan, like *Pleurobrachia*, the behaviors of these two species are remarkably different. *Euplokamis* shows a characteristic fast escape swimming mediated by very long swim cilia—the longest swim cilia in ctenophores measured as a ratio to the body size. Unusual tentacles with coiled tentilla and striated muscles are also unique innovations of *Euplokamis* (Mackie et al., 1988; Mills, 1987). Notably, those striated muscles are used to actively extend tentilla on contact with copepod preys. On the other hand, the recoiling of tentilla is a passive process mediated by specific internal collagen springs. In *Euplokamis*, the overall integration of behaviors and comb ciliary activity is presumably mediated by the aboral organ as in other ctenophores (Tamm, 1982; Tamm, 2014). Figure 1 shows the relationships among ctenophores used in this study, with a position of *Euplokamis* as a sister lineage to the rest of ctenophores (Moroz et al., 2014; Whelan et al., 2015; Whelan et al., 2017).

3.2 | The Aboral sensory complex

In *Euplokamis*, similarly to *Pleurobrachia* and *Beroe* (Jager et al., 2011; Norekian & Moroz, 2019a, 2019b), the tubulin antibody specifically labeled neuronal elements and different types of cilia. Thus, tubulin immunoreactivity (IR) together with phalloidin staining of F-actin in muscle fibers provided a good overview of the entire aboral complex area.

We reliably visualized the aboral organ itself, two narrow polar fields similar in their shape and appearance to polar fields of *Pleurobrachia*, eight ciliated furrows connecting comb rows to the

aboral organ and two brightly stained tentacular nerves approaching, but not directly connecting to the aboral organ (Figure 2). We also identified comb row nerves (Figure 2a; see text below)—the feature unique to the fast-moving *Euplokamis* (Mackie et al., 1992) but not to other studied species.

Phalloidin labeled numerous muscle fibers inside the walls of the aboral canal; those fibers extended from the pharynx to the aboral end of the animal. Very powerful radial muscles connected the aboral canal to the outer walls of *Euplokamis* (Figure 2).

3.3 | The subepithelial neural network

Tubulin IR in *Euplokamis* revealed the wide-spread subepithelial neural net, which covered the entire surface of the body. It consisted of a distributed polygonal mesh of neural processes forming units of different sizes (between 20 and 150 μ m) and shapes in mostly quadrilateral (four corners), pentagonal (five corners), hexagonal (six corners), and heptagonal (seven corners) configurations (Figures 3 and 4).

The strands of the neural network contained numerous nuclei stained by DAPI, indicating that the neural somata that form the network are located within its strands (Figure 3a,b). In addition to the strands of the mesh, the subepithelial network included separate neurons in the same focal plane. These neurons were 3–6 μ m in diameter and produced multiple neurites, which frequently joined the processes in the polygonal mesh contributing to its structure (Figure 3a,b). Some of the processes terminated in the space between network threads.

3.4 | Tentacular nerves

Euplokamis, like other cydippid ctenophores, uses two tentacles with numerous tentilla to catch the prey. And, like in *Pleurobrachia*, tubulin IR revealed four tentacular nerves, two on each side of the animal, controlling the movements of the tentacles.

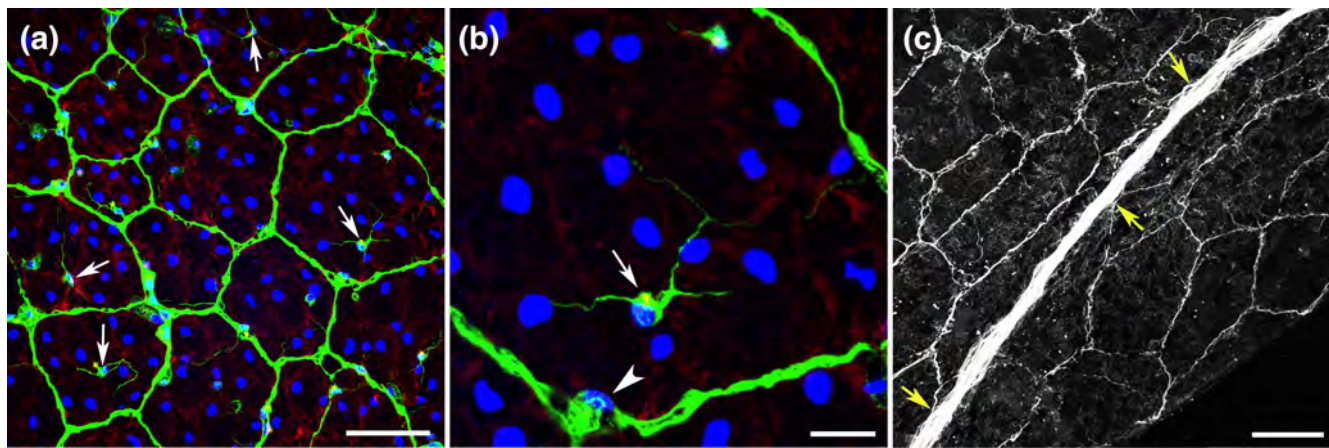


FIGURE 3 Subepithelial neural network in *Euplokamis* stained with tubulin antibody (green, while nuclear DAPI labeling is blue). a, A neural net consists of polygonal units of different shapes and sizes. There are also individual neurons (arrows) between network strands with multiple neurites, some of which are joining the network. b, High magnification focusing on one of the neurons between network strands (arrow) and cell nucleus inside the strands (arrowhead). c, The tentacular nerve is composed of numerous tightly packed thin neurites and intertwines with the polygonal network (arrows show direct connections between the nerve and network). Scale bars: a: 40 μ m; b: 10 μ m; c: 50 μ m [Color figure can be viewed at wileyonlinelibrary.com]

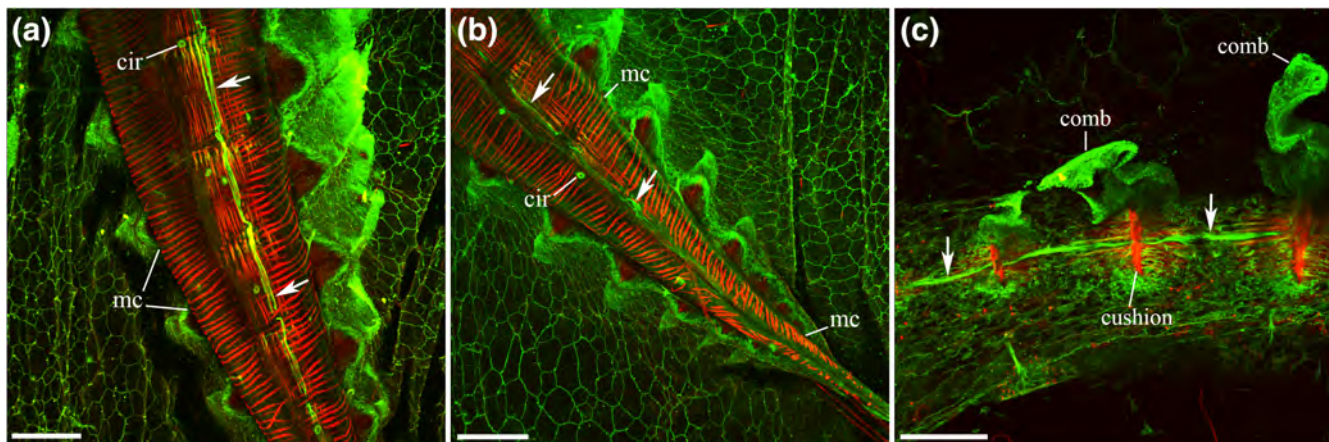


FIGURE 4 The comb row nerve in *Euplokamis* (tubulin IR is green; phalloidin staining is red). a, b, The horizontal view of the comb row with the nerve (arrows) running longitudinally in the center of the row. All images reveal the polygonal neural network, covering the entire surface. Phalloidin labels numerous parallel rings of muscle fibers tightly encircling the meridional canal (mc), which runs under each comb row. Each meridional canal contains a row of small pores or ciliated rosettes (cir), along its length, which are brightly stained by tubulin antibody. c, The sagittal view of the comb row with the nerve (arrows) running right under the comb plates. Note that swim cilia are also labeled by tubulin antibody (green), while the combs base cushion is stained by phalloidin (red). Scale bars: a, b: 200 μ m; c: 50 μ m [Color figure can be viewed at wileyonlinelibrary.com]

Two *aboral* tentacular nerves approached the aboral organ from both sides (Figure 2a). These nerves branched, became thinner and merged with the surface network without visible direct connection to the aboral organ (Figure 2a). On the other end, the nerves ran into the ipsilateral tentacle pockets and innervated each tentacle. Two *oral* tentacular nerves originated on both sides of the mouth and continued to the ipsilateral tentacle pockets. Each tentacular nerve consisted of numerous thin processes tightly packed together (Figure 3c). The nerves were located in the same focal plane as the subepithelial neural network and had many direct connections with it through its entire length closely intertwining with the network (Figure 3c). Thus, tentacular nerves appeared to be a

part of the entire surface network, collecting information from the surface and transmitting it into the tentacle pocket and vice versa to coordinate the tentacle movements.

3.5 | Comb row nerves

One feature, unique to *Euplokamis*, is an unusually fast escape swimming, which is mediated, at least partially, by a system of “giant axons” running longitudinally along each of eight comb rows (Mackie et al., 1992). Tubulin IR revealed a single comb row nerve consisting of several processes right under the cushion of swim plates, above the underlying meridional canal, and in the same

subepithelial layer as the rest of the diffused network (Figures 4 and 5a,b). Upon approaching the aboral end of the animal, when the comb rows ended, the nerve continued under the ciliated furrow directly to the aboral organ (Figure 4c and 5b). This type of comb nerves was never observed in other ctenophores (Hernandez-Nicase, 1991; Jager et al., 2011; Jager et al., 2013; Norekian & Moroz, 2016, 2019a, 2019b). For example, in *P. pileus*, the regular subepithelial neural network could be seen in the comb rows between individual comb plates with no traces of any axons running along the row (Figure 13c).

As was shown in *Pleurobrachia*, at earlier developmental stages ctenophores have only 4 comb rows, while in older larva each of the four begins to split into two "sister" rows to form 8 rows in adults (Norekian & Moroz, 2016). In *Euplokamis*, we have found that two comb row nerves (which followed these two "sister" comb rows and then ciliated furrows) joined each other upon entering the aboral organ (Figure 5C,D). Each nerve divided, with one branch continuing to the aboral organ, while another branch was making a loop and joining the "sister" nerve (Figure 5c,d; Supplement Video 1). This morphological organization suggests that two neighboring nerves and comb rows can closely and directly coordinate their activity bypassing such central distributing structure as the aboral sensory organ.

3.6 | Neurons of mesoglea

The second major part of the *Euplokamis* neural system is a web of neurons and fibers spread over the entire internal gelatinous part of the body—mesogleal area (Figure 6a). The neuronal cell bodies had a size varying between 5 and 10 μ m and could be separated into four types of cells, based on their processes' patterns. The most numerous cells were bipolar neurons with two neurites on opposite sides of the somata (Figure 6b). The second type consisted of neurons with three main neurites—tripolar neurons (Figure 6c,d). There were also numerous multipolar neurons with elongated processes projecting in different directions (Figures 6e,f). The fourth type of cells had long thin filament-type processes crossing the large areas of the mesogleal space. *Pleurobrachia* appeared to have more multipolar star-like neurons in the mesoglea (*P. pileus*, – Figure 12F; *P. bachei* – (Norekian & Moroz, 2019b).

3.7 | Surface receptors

We identified three types of putative sensory cells, which were visualized on the body surface of *Euplokamis* (Figure 7a,b).

The first receptor type had a long and thick single cilium up to 10 μ m in length. Similar sensory cells, presumably mechanoreceptors, have also been identified in other ctenophores (Norekian & Moroz,

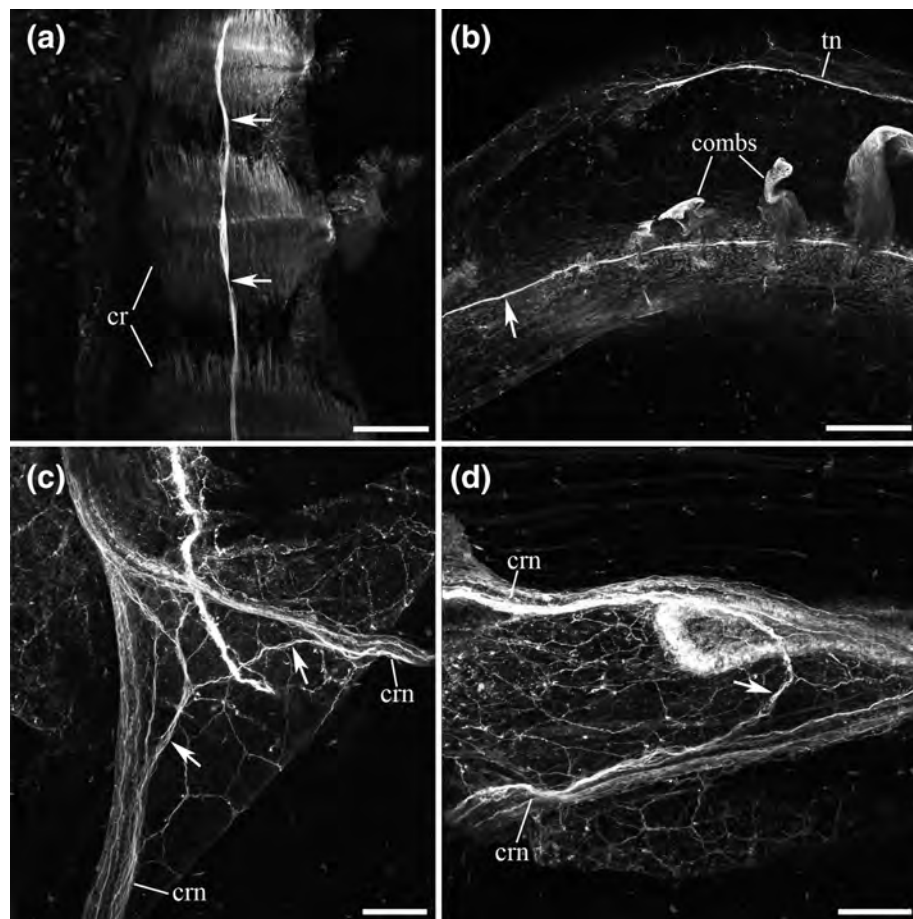


FIGURE 5 Comb row nerves in *Euplokamis* labeled by tubulin antibody. a, The horizontal view of the comb row (cr) with the nerve indicated by arrows. b, Sagittal view of the comb row, which is ending next to the aboral pole of the animal. The comb row nerve (arrow) continues toward the aboral organ. The tentacular nerve (tn) is also visible. c, d, Two neighboring comb row nerves (crn) approach the aboral organ complex. Some of the neurites from each nerve continue toward the aboral organ, while others form a looping branch that connects two "sister" nerves (arrows). See also video in Supplement S1. Scale bars: a, c: 100 μ m; b, d: 200 μ m

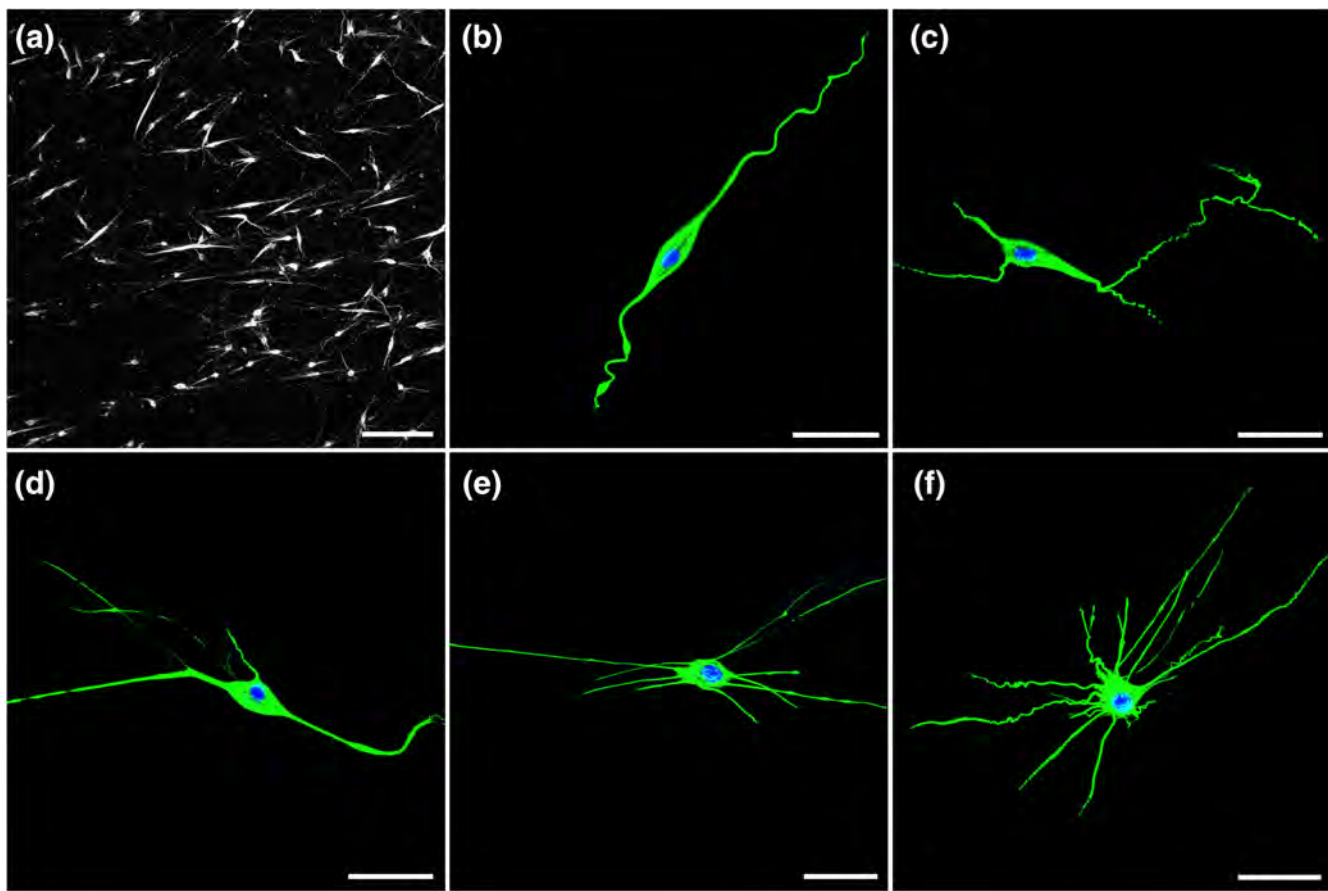


FIGURE 6 *Euplokamis* mesogleal neurons stained by tubulin antibody (green, while nuclear DAPI labeling is blue). a, Mesogleal region is packed with neuronal cells. b, The most numerous cell type is bipolar neurons with processes on opposite poles of the cell. c, d, Tripolar neurons with three main processes. e, f, Multipolar neurons, including star-like neurons projecting processes in all directions. Scale bars: a: 100 μ m; b-f: 20 μ m [Color figure can be viewed at wileyonlinelibrary.com]

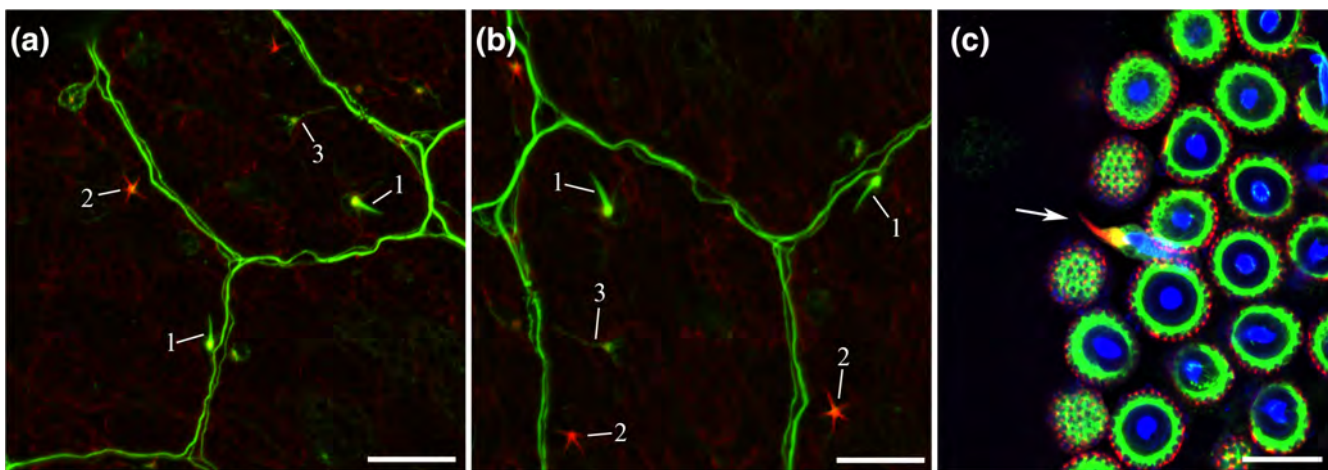


FIGURE 7 In *Euplokamis*, three types of receptors are found on the surface of the skin using tubulin IR (green), phalloidin (red), and nuclear DAPI (blue) labeling. a, b, The first receptor type (1) has a single large and thick cilium brightly stained by tubulin antibody, located on the top of tubulin IR cell with processes. The second type of sensory cells (2) contains a compact group of 2 to 8 stereocilia labeled by phalloidin. The third type of receptors (3) has a very thin cilium that is weakly stained by tubulin antibody. c, Tentilla also have receptor cells among colloblasts with one or more stereocilia labeled by phalloidin (arrow). Scale bars: a: 20 μ m; b: 15 μ m; c: 10 μ m [Color figure can be viewed at wileyonlinelibrary.com]

2019a, 2019b). However, there was one significant difference. In *Pleurobrachia* and *Beroe*, their single stereocilium was always brightly labeled by phalloidin. In *Euplokamis*, the similar/homologous structure was brightly stained by tubulin antibody, suggesting true ciliated nature in its molecular makeup (Figure 7a,b). One additional distinction—the relative length of the cilia, as related to the body size, was the largest in *Euplokamis* compared to all studied ctenophores.

The second receptor type was represented by cells with a tight group of 2 to 8 stereocilia, 3–7 μm length, projecting in different directions but connected to a single base (Figure 7a,b). These stereocilia were brightly stained by phalloidin. Similar receptors were found in *Pleurobrachia* and *Beroe*, although in *Beroe*, the stereocilia were much bigger (Norekian & Moroz, 2019a, 2019b).

The third receptor type had a single, very thin cilium, about 10 μm length, located at the apical part of the cells, about 5 μm in diameter (Figure 7A,B). This type of cilia was weakly marked by tubulin IR (Figure 7A,B). A similar receptor type was also found in *Pleurobrachia* and *Beroe* (Norekian & Moroz, 2019a, 2019b).

Euplokamis tentacles and tentilla also had on their surface, among colloblasts, numerous sensory cells with a single stereocilium labeled

by phalloidin (Figure 7c). Some of them had several, up to 4, phalloidin-labeled stereocilia. Similar receptors with a single stereocilium were also found in the tentacles of *Pleurobrachia* (Norekian & Moroz, 2019b).

3.8 | The muscular system

Phalloidin labeled several different muscle groups in *Euplokamis*. Specifically, it stained numerous thin longitudinal filaments in the walls of the aboral canal (Figure 8d,e), and muscle filaments attached to the outside integument or wall of the pharynx (Figure 8A). It also labeled long and thin circular and longitudinal muscle fibers crossing the entire body of *Euplokamis*, as in *Pleurobrachia* (Norekian & Moroz, 2019b). One striking difference from *Pleurobrachia* was a large number of very powerful bundles of radial muscles, crossing the mesoglea and connecting the outer wall with the aboral canal in *Euplokamis* (Figure 2a and 8b-e). These muscle fibers were much thicker than the rest of mesogleal muscles and branched extensively at the point of attachment (Figure 8c-e).

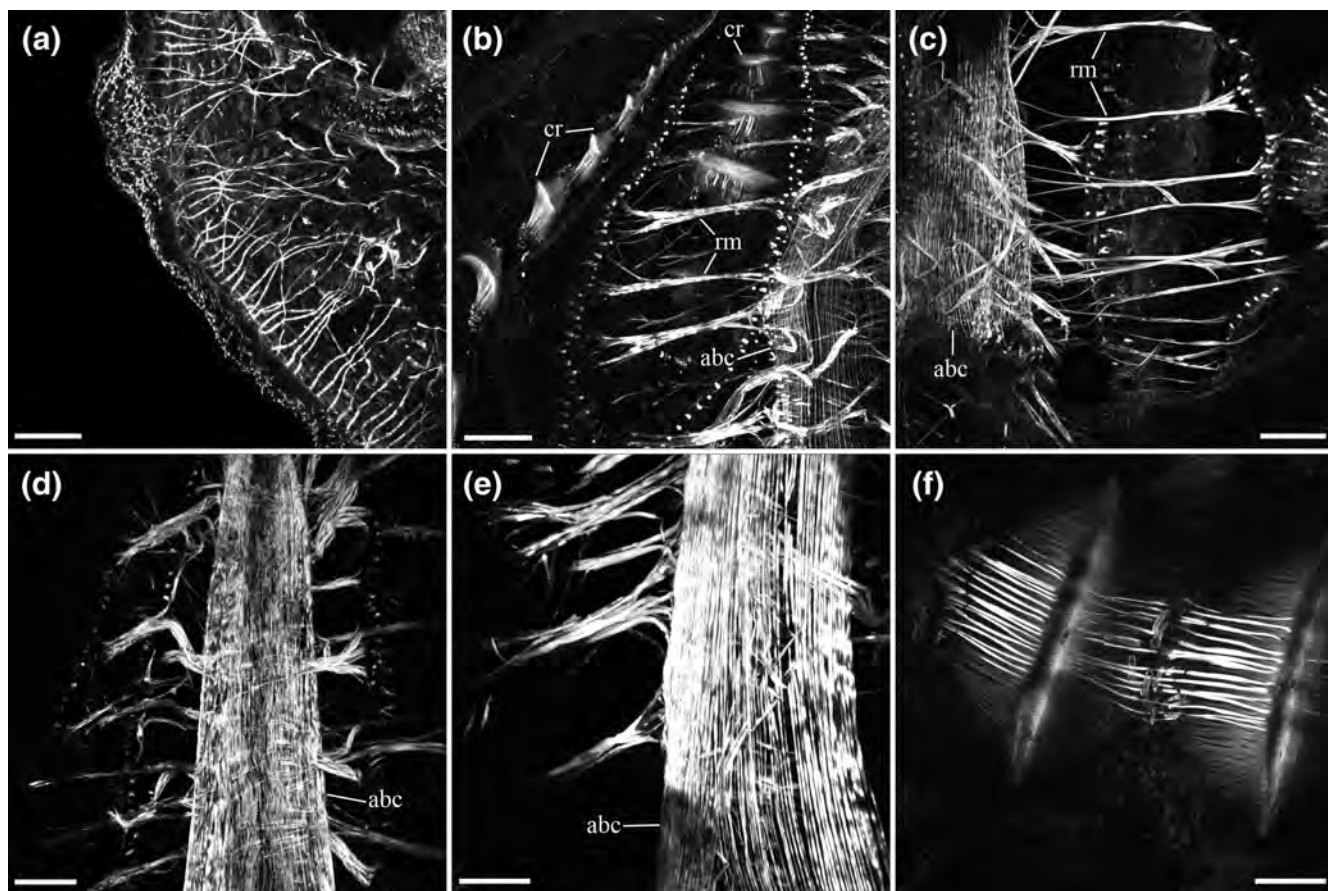


FIGURE 8 The diversity of muscle groups in *Euplokamis* stained by phalloidin. a, Thin muscle filaments attached to the integument. b, c, The “powerful” bundles of radial muscles (rm) cross the mesoglea and connect the aboral canal (abc) with outside body wall that carries comb rows (cr). d, e, Each bundle of radial muscles consists of 5 to 10 individual fibers and firmly attaches to the aboral canal wall. The thin wall of the aboral canal itself has numerous longitudinal muscle fibers running in parallel through its entire length. f, Comb rows have groups of short muscle fibers, which connect neighboring comb plates. Scale bars: a: 100 μm ; b, c: 200 μm ; d: 150 μm ; e, f: 100 μm

Phalloidin staining also revealed groups of short non-contractile muscle fibers connecting neighboring comb plates in *Euplokamis* (Figure 8f). Similar structures were also detected in *Pleurobrachia* and *Beroe* (Norekian & Moroz, 2019a, 2019b). Numerous flat muscle fibers were tightly encircling each meridional canal, forming dense parallel rings, which became smaller as each canal was getting thinner at its ends (Figure 4a,b). This pattern is very distinct to *Euplokamis* and never detected in other ctenophores studied so far. Meridional canals also contained labeled by tubulin IR pores or ciliated rosettes found in all studied ctenophores (see Hernandez-Nicase, 1991), which lined up along their entire length and connected the gastrovascular canal system with mesoglea (Figure 4a,b).

In *Euplokamis*, each tentacle possesses 10–50 side branches or tentilla usually coiled into tight spirals (Mills, 1987). The entire main trunk of tentacles was intensively labeled by phalloidin confirming its muscular nature (Figure 9a). Each tentilla had at least seven individual strands of muscle fibers brightly stained by phalloidin and tightly packed together (Figure 9b,c). In *Pleurobrachia*, we saw only two strands of phalloidin-labeled fibers inside each tentilla (Norekian & Moroz, 2019b).

The tentilla of *Euplokamis* differ significantly from those of other cypiddids: they contain striated muscles along with conventional

smooth muscles (Mackie et al., 1988). However, the striation of phalloidin-labeled muscle fibers in tentilla was not visible in our confocal microscopy images (Figure 9d). The striated muscles control the fast discharge of tentilla during prey capture—a very quick uncoiling movement produced by contraction of the striated muscles located on the outside of the coil (Mackie et al., 1988). Several rows of collagen-containing “boxes” presumably provide structural support for the tentilla during contraction of striated muscles (Mackie et al., 1988). Tubulin IR staining revealed several long neuronal processes (axons) running in parallel along each row of “boxes” just under the phalloidin-labeled muscle fibers (Figure 9e,f). They appear to be unique to *Euplokamis* and have not been seen in *Pleurobrachia*.

3.9 | Pharynx cilia

All studied ctenophore species have numerous cilia covering the inner surface of their mouth and pharynx. In *Euplokamis*, both the mouth and pharynx were also outlined by thin cilia arranged in groups. Each group was stained by tubulin IR and was attached to a bundle of noncontractile actin filaments brightly labeled by phalloidin (Figure 10a). Similar bundles of phalloidin-labeled actin filaments have been originally described at the base of the macrocilia in *Beroe* (Tamm, 2014; Tamm & Tamm, 1987) and

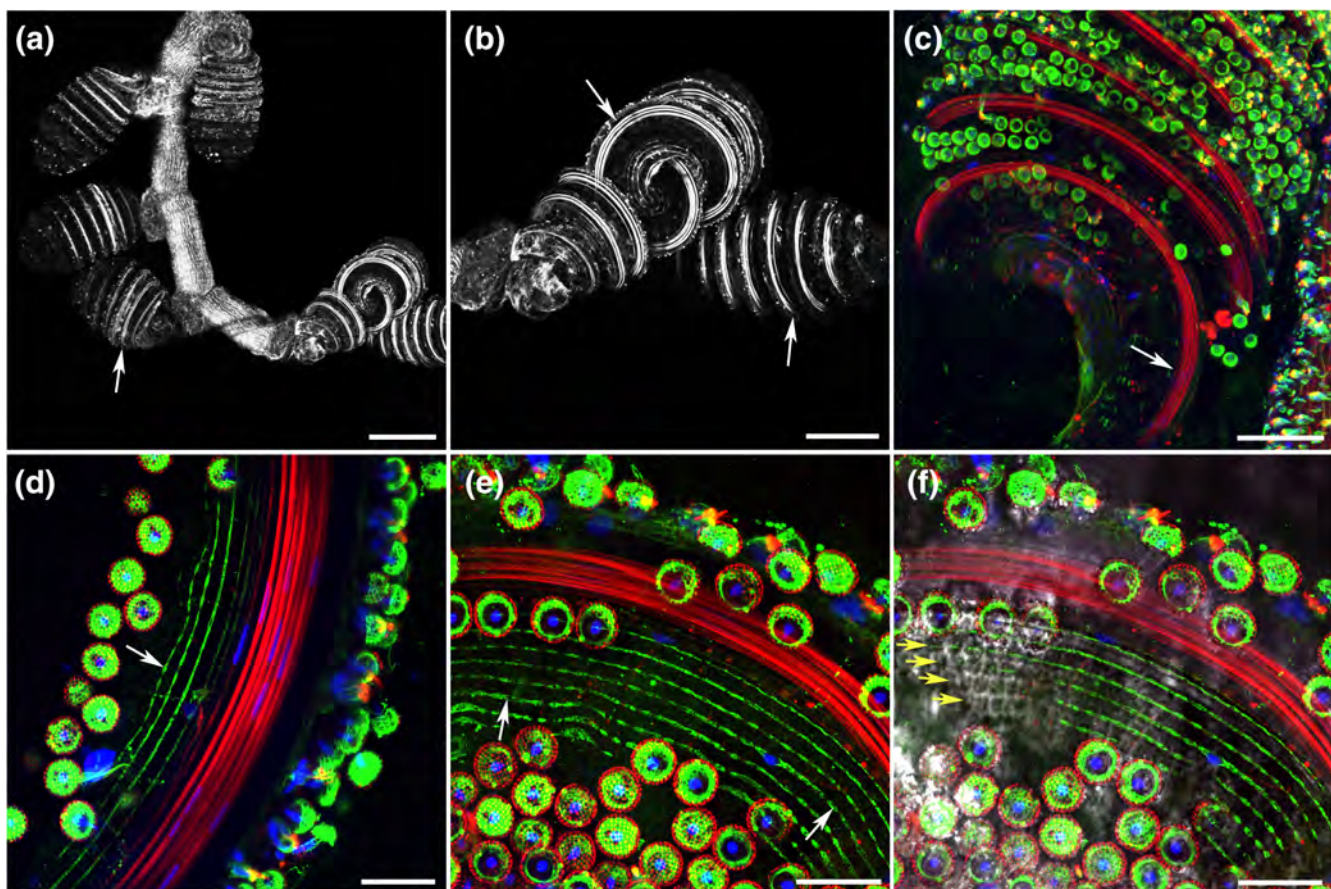


FIGURE 9 The muscular system of the tentacles in *Euplokamis*. a, Phalloidin labels the entire main trunk of each tentacle. b, It also labels muscle fibers in each tentilla (arrows). c, d, Each tentilla has several strands of muscle fibers (at least 7), which are usually packed in tight spirals (red). The tentilla are covered with colloblasts that are labeled by tubulin antibody (green); DAPI nuclear labeling is blue. e, f, Tubulin IR also labeled several neuronal processes (white arrows in d, e) running parallel to the muscle fibers and along the “box” rows (yellow arrows), which provide structural support for tentilla and could be better seen with transmitted light differential interference contrast channel (f). Scale bars: a: 200 μ m, b: 100 μ m, c: 50 μ m, d, e, f: 20 μ m [Color figure can be viewed at wileyonlinelibrary.com]

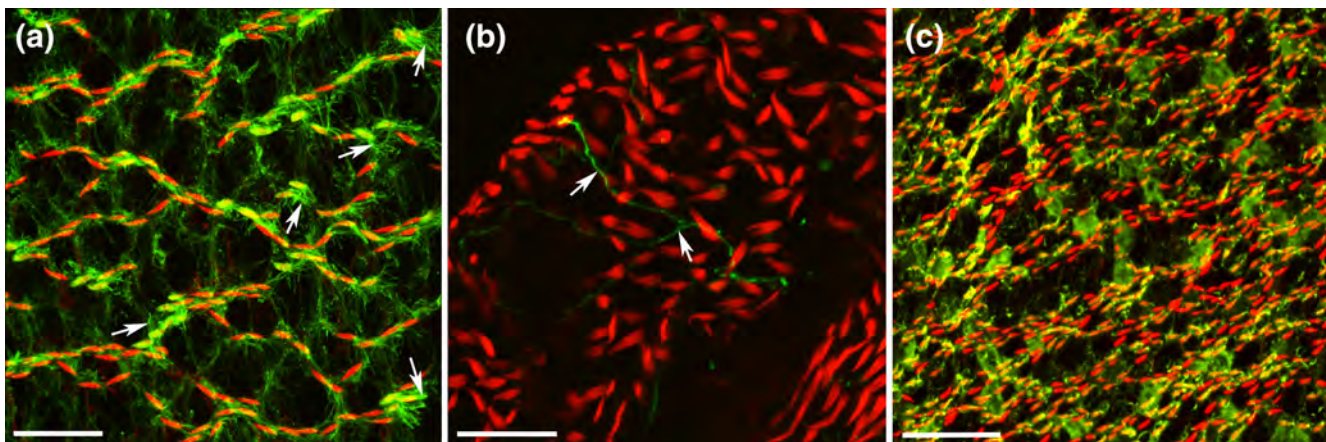


FIGURE 10 Cilia are outlining the surface of the pharynx. Phalloidin (red) labels bundles of actin filaments at the roots of thin cilia, which are visualized by tubulin IR (green). a, Pharynx of *Euplokamis*—groups of tubulin IR cilia are indicated by arrows. b, Pharynx of *Bolinopsis*—Tubulin IR labeling of cilia is too weak and not visible. Arrows indicate neural processes in the pharynx wall. c, Pharynx of *Hormiphora*. Scale bars: a: 30 μ m, b: 20 μ m, c: 60 μ m [Color figure can be viewed at wileyonlinelibrary.com]

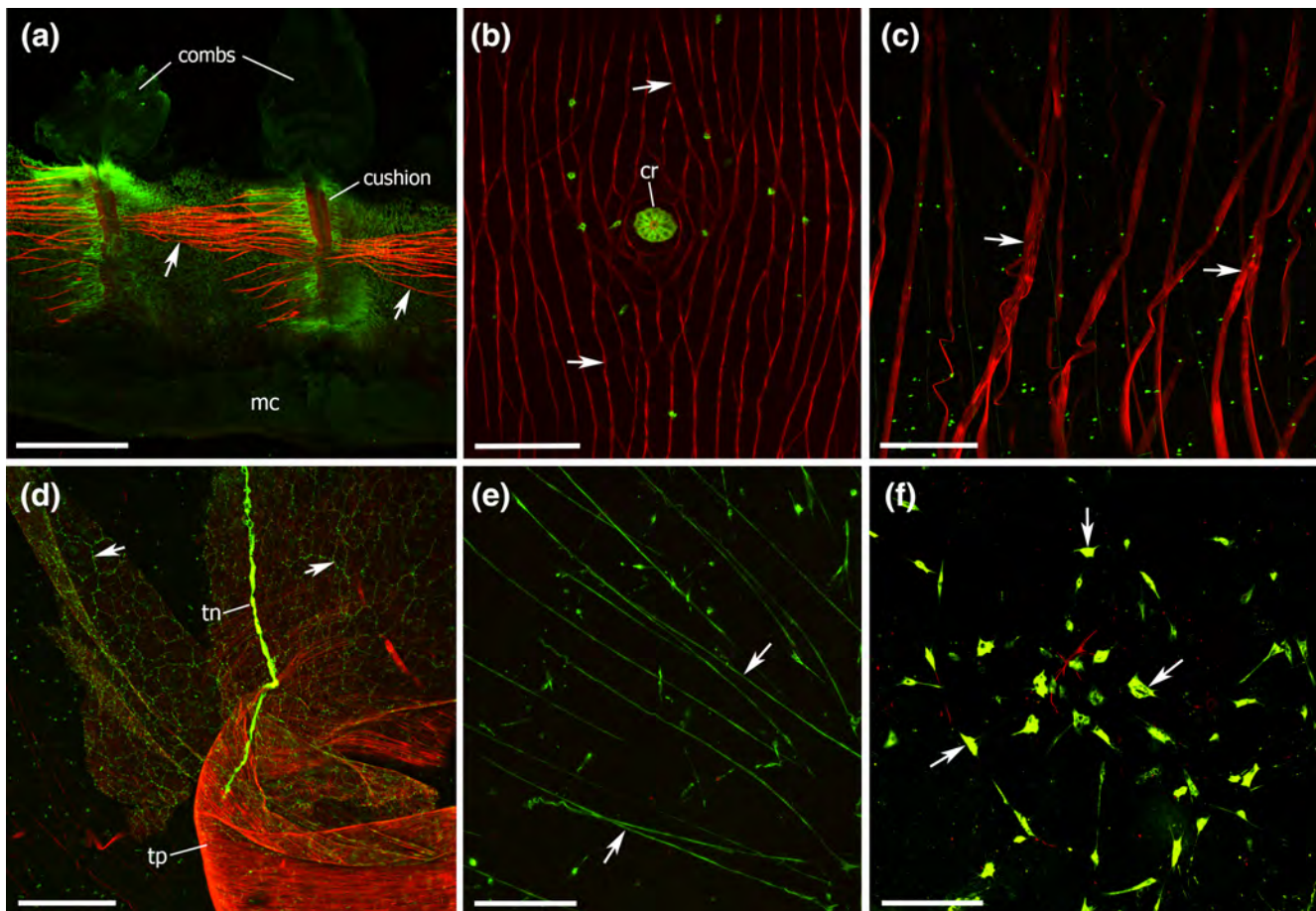


FIGURE 11 Phalloidin (red) and tubulin IR (green) labeling in *Hormiphora*. a, Noncontractile muscle fibers (arrows) in comb rows connecting neighboring cushions. b, Ciliated rosette (cr) in the meridional canal. Note the network of phalloidin-labeled fibers in the walls of the canal (arrows). c, Long muscle fibers (arrows) that are attached to the comb rows and extend into the mesoglea. d, Tentacle nerve (tn) is approaching the tentacle pocket (tp). Arrows show the subepithelial neural network labeled by tubulin IR. e, Numerous neural processes (arrows) labeled by tubulin IR cross the mesogleal region. f, Mesogleal region also contains several neural cell bodies (arrows, labeled by tubulin IR). Scale bars: a, d: 400 μ m; b: 50 μ m; c: 300 μ m; e: 200 μ m; f: 80 μ m [Color figure can be viewed at wileyonlinelibrary.com]

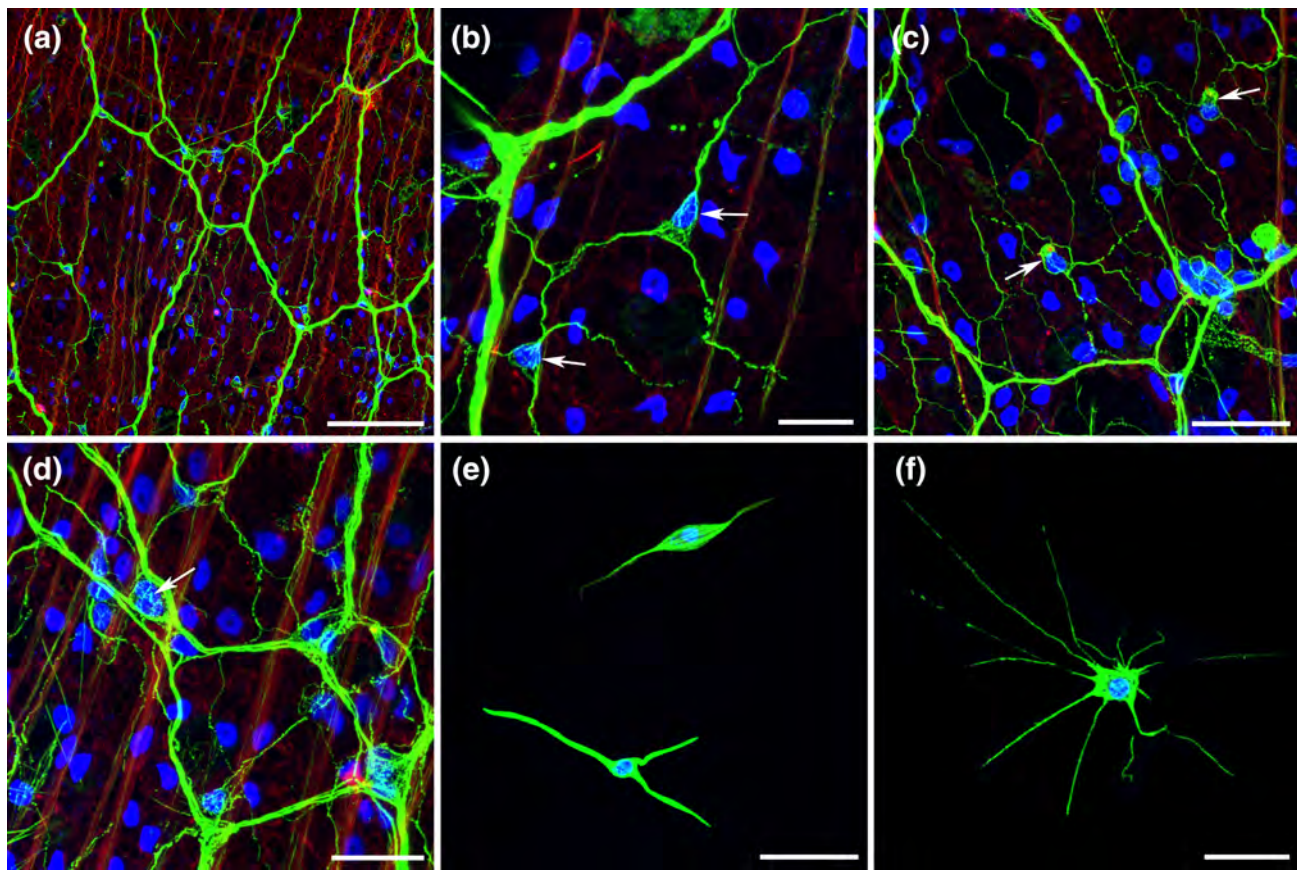


FIGURE 12 The neural system of *Pleurobrachia pileus* (tubulin IR is shown in green, phalloidin staining is red, while nuclear DAPI is blue). a, Subepithelial neural network. Parietal muscle fibers (red) are located just under the neural net. b, Individual neurons (arrows) with long processes are also seen between the major strands of the network. c, Some of the free-standing inter-network neurons are sensory cells (arrows). d, Numerous nuclei could be seen in the strands of the network (arrow). Note that the strands represent the bundles of separate thin neural fibers. e, Bipolar and tripolar neurons in the mesogleal area. f, Large multipolar star-like neuron in the mesoglea. Scale bars: a: 50 μ m; b: 10 μ m; c: 20 μ m; d: 15 μ m; e, f: 20 μ m [Color figure can be viewed at wileyonlinelibrary.com]

later shown at the roots of groups of thin cilia in the pharynx of *Pleurobrachia* and *Beroe* (Norekian & Moroz, 2019a, 2019b). Those phalloidin-labeled actin filaments at the roots of thin pharynx cilia were found in all studied species, including *Bolinopsis* (Figure 10b) and *Hormiphora* (Figure 10c). The pharynx cilia were stained by tubulin IR very weakly and sometimes were not even visible, while phalloidin-labeled roots always brightly outlined the walls of the pharynx.

3.10 | Comparative overview of neural networks and muscles across ctenophores

According to our screening, the basic neural architecture is highly conservative across the entire Ctenophore phylum. All studied species had a similar polygonal subepithelial neural network covering the entire surface of the body. For example, the subepithelial network in the cydippid *H. hormiphora* was very similar to the network in *Pleurobrachia bachei* (Norekian & Moroz, 2019b); there were only slightly larger sizes of individual neurons and network units (which was expected because of superior body size of *Hormiphora*—Figure 11).

The nervous system of *P. pileus* collected in the Black Sea was almost indistinguishable from the Pacific *P. bachei* with identical

in size polygonal units of subepithelial neural network and individual neurons located between the main strands, as well as sensory neurons with a single short cilium (Figure 12a-d). The mesogleal area contained the same types of neurons labeled by tubulin antibody, including bipolar, tripolar, and multipolar star-like cells (Figure 12E,F). We noticed a significant number of multipolar star-like neurons located very close to the subepithelial network, with their processes seemingly making direct contact with the net (Figure 13a).

Similarly, tubulin IR in a highly derived cydippid *D. glandiformis* revealed the same type of polygonal network consisting of various units with sizes between 20 and 150 μ m and individual neurons between strands of the net (Figure 14).

Furthermore, *B. infundibulum*, a representative of the different order Lobata, also had a similar structure of a subepithelial polygonal neural network covering a large part of its surface (Figure 15a,b). The size of the polygonal units was between 30 and 300 μ m, which reflected its much larger body size. However, there was one important deviation from the conservative architecture of subepithelial network in the large feeding lobes of Lobata. The neural net in those areas consisted only of large rectangular units of

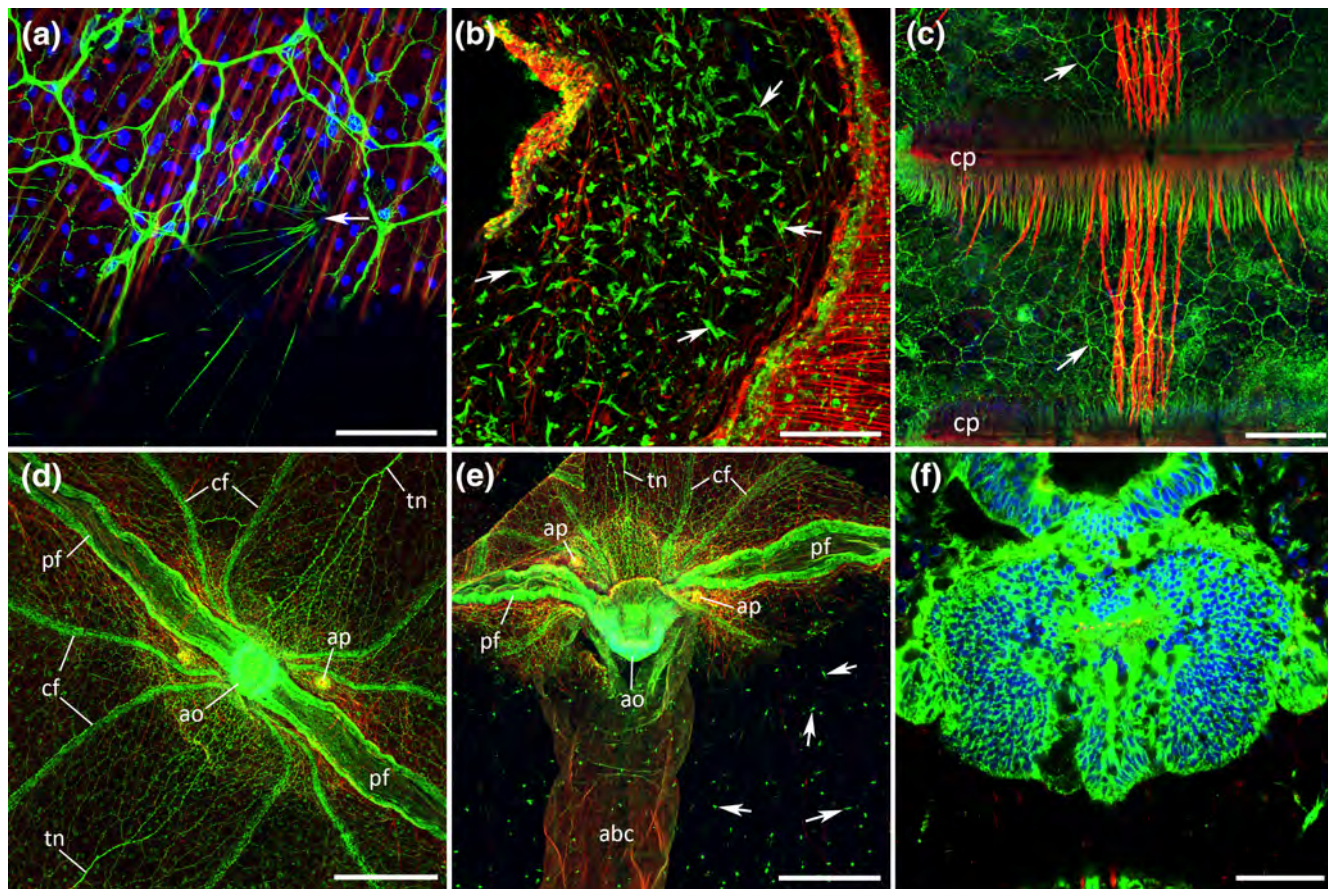


FIGURE 13 The neural system of *Pleurobrachia pileus* (2). a, Some of the numerous multipolar star-like neurons from mesoglea (arrow points to the position of the cell body) are located very close to the subepithelial network. Their multiple long processes also project in the direction of subepithelial neural network and could have a physical connection with it. b, Optical cross-section through the lips reveals an unusually high density of large mesogleal neurons (arrows show some) in that area. c, Unlike *Euplokamis*, *Pleurobrachia* does not have any large axons along the comb rows—only the regular subepithelial network (arrows) is crossing each comb row between the plates. d, Horizontal view of the aboral organ and polar fields. Note the subepithelial neural network and two tentacular nerves. e, Side view of the aboral organ area. Arrows point to numerous small mesogleal neurons. f, Aboral organ is always brightly stained by tubulin antibody and represents a tightly packed group of IR cells, presumably neurons. *abc*, aboral canal; *ap*, anal pore; *ao*, aboral organ; *cf*, ciliated furrow; *cp*, comb plate; *pf*, polar field; *tn*, tentacular nerve. Scale bars: a: 50 μ m; b, c: 100 μ m; d, e: 300 μ m; f: 60 μ m [Color figure can be viewed at wileyonlinelibrary.com]

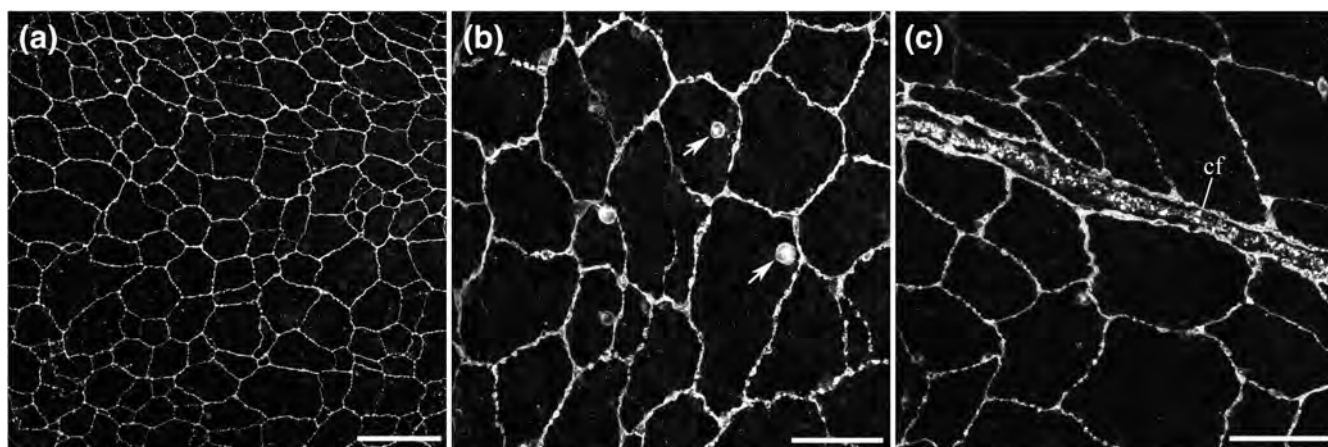


FIGURE 14 Subepithelial neural network labeled by tubulin antibody in *Dryodora*. Individual neuronal somata are located between the network strands (arrows). Ciliated furrow (cf) is tightly framed by the net in (c). scale bars: a: 200 μ m; b, c: 75 μ m

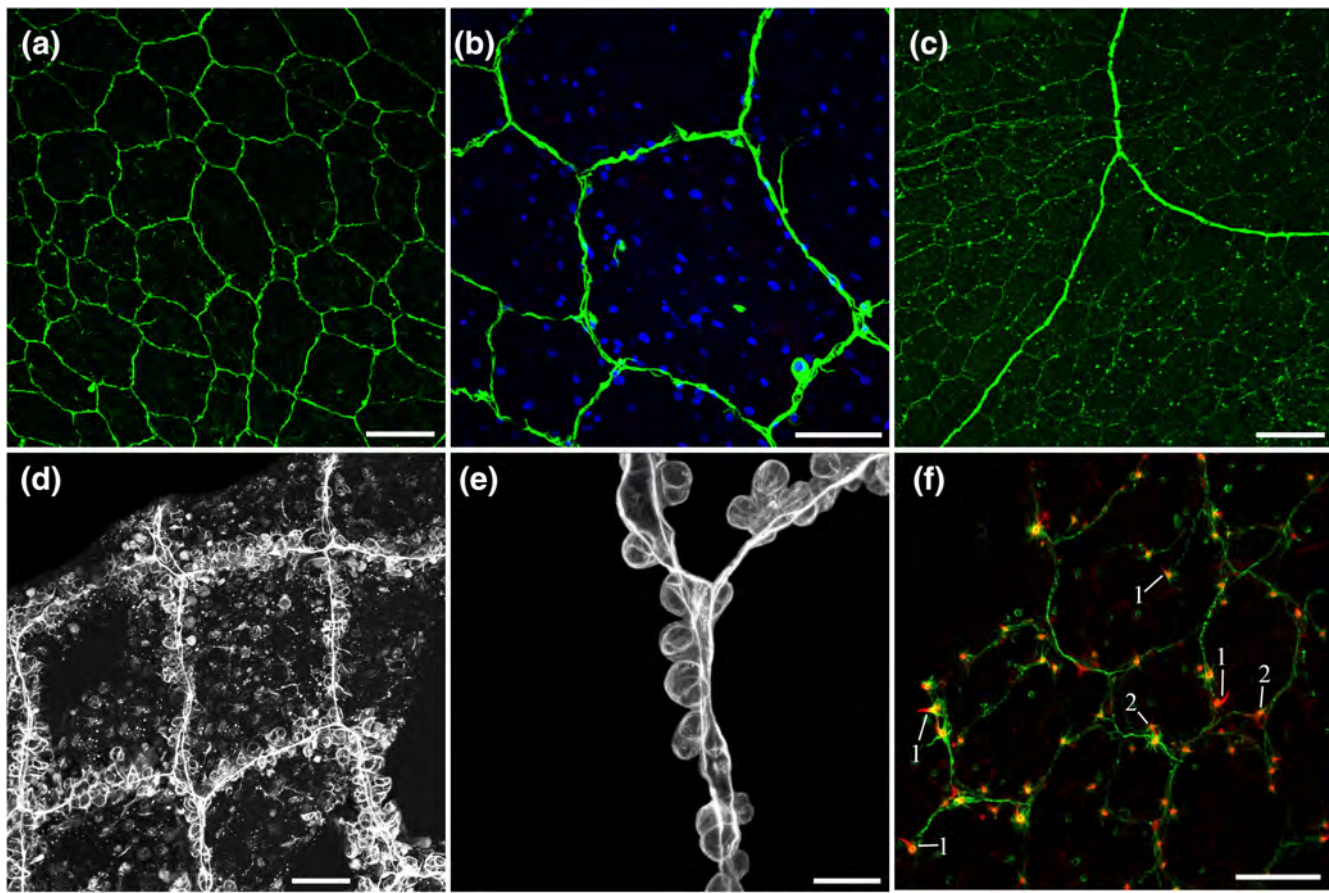


FIGURE 15 Neural network labeled by tubulin antibody in *Bolinopsis*. a, b, Subepithelial neural network in the body wall has a typical polygonal structure. c, Some of the network strands are much thicker and look like branching nerves. d, In the feeding lobes of *Bolinopsis*, the network forms large rectangular units. e, There are numerous round-shaped neuronal-like somata associated with the strands of this rectangular meshwork. f, Surface receptors in *Bolinopsis* stained by phalloidin (red) and tubulin antibody (green). Receptors of the first type have a single stereocilium (1) and receptors of the second type have multiple stereocilia (2). Scale bars: a: 100 μ m; b: 40 μ m; c: 200 μ m; d: 50 μ m; e: 20 μ m; f: 60 μ m [Color figure can be viewed at wileyonlinelibrary.com]

100–200 μ m sizes (Figure 15D). The strands of the mesh were covered with large (about 10 μ m) round-shaped tubulin IR cell bodies, which looked like grapes on the vine (Figure 15e). Another lobate ctenophore *M. leidyi*, which is a close relative of *Bolinopsis*, had the identical network polygonal structure in the body wall, and square/rectangular mesh on the inner surface of the feeding lobes (Figure 16b–e). Numerous tubulin IR round-shaped cells (up to 10 μ m in diameter) were tightly attached to the strands of the rectangular network (Figure 16f). This square/rectangular network on the inner surface of the feeding lobes with round cell bodies was visible also under the stereo (light) microscope even without tubulin IR staining (Figure 17a–c).

One significant feature in *Mnemiopsis* (unlike *Bolinopsis*) is that adult animals maintain tentacles after the cydippid larva stage, which are still used in feeding. The tentacle sheaths disappear in adults, and on both sides of the tentacle bulb, ciliated auricular grooves are formed, which guide the reduced tentacles in adults. The cilia in the grooves, which are brightly labeled by tubulin antibody (Figure 18), create currents that carry small zooplankton collected by tentacles to the mouth.

B. ovata is closely related to *B. abyssicola* (Norekian & Moroz, 2019a). The body of *B. ovata* is very flat compared to more rounded *B. abyssicola* and has more yellowish coloration. Two features, known to be unique to Beroid species, were also found in *B. ovata*: (a) sharp and stiff macrocilia in the mouth that helps to grab the pieces of a large prey (Figure 19c), and (b) polar fields with a crown of large protruding lobes covered with long cilia (Figure 19E,F and Supplement Video S2). These long cilia were brightly stained by tubulin antibody, providing good visualization of the polar fields in IR preparations (Figure 20).

There were also individual neuron-like cell bodies labeled by tubulin IR in the center of polar fields between the lobes (Figure 21c). A subepithelial neural network consisting of polygonal units of different sizes covered the entire outer surface of *B. ovata* (Figure 21). Similarly to *B. abyssicola* (Norekian & Moroz, 2019a), the entire surface of the pharynx was also covered by subepithelial network effectively doubling the network size. Mesogleal area was filled with neurons of different types, bipolar cells being the most abundant (Figure 21e,f).

The receptors were detected in several species of ctenophores—*D. glandiformis*, *B. infundibulum*, *M. leidyi*, and *B. ovata*. In all species, we

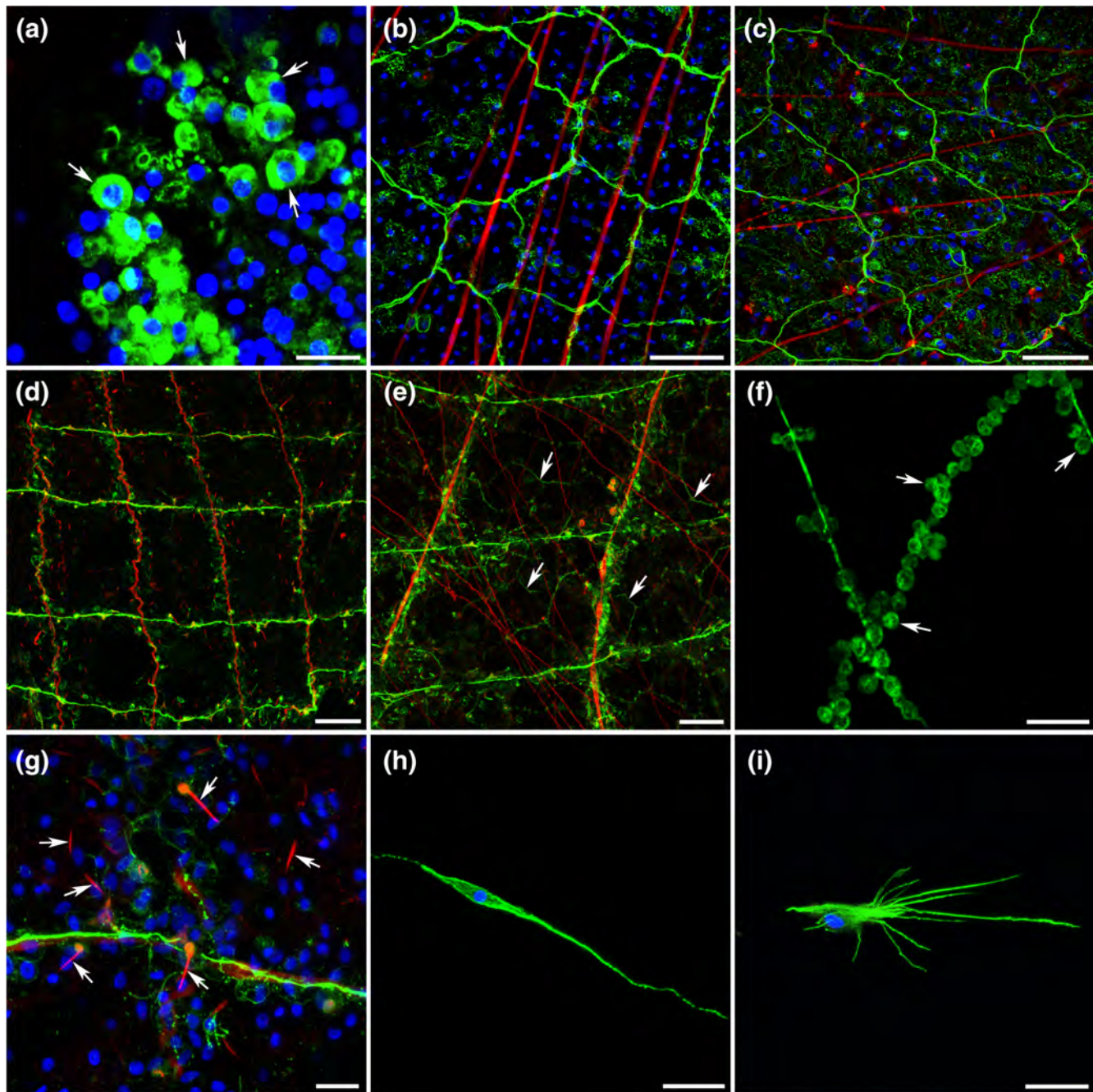


FIGURE 16 Tubulin antibody labeling (green) of the neural system of *Mnemiopsis*. Phalloidin staining is red, while DAPI is blue. a, Cells brightly labeled by tubulin antibody in the aboral organ (arrows). b, Subepithelial neural network in the body wall. Phalloidin (red) labels muscle fibers. c, Auricles (four small lobes around the mouth) have a similar subepithelial neural network as in the body wall. d, A rectangular-shape neural network in the feeding lobes. Note that neural (green) and muscle (red) fibers run together in the same pattern. There were no “canonical” polygonal units in this area. e, At the base of the feeding lobes, rectangular units are much larger (compare to d). Neural processes forming polygonal units (arrows) can also be seen at the base of the lobes. f, Clusters of round-shaped cells along the lines of a rectangular network of the feeding lobes (arrows show some cells). g, There is a very high density of single cilium mechanoreceptors (arrows show some) on the inside surface of the feeding lobes. This high density is observed closer to the edge and in the middle of the lobes (as in d) but not at the very base (as in e). h, i, Bipolar and multipolar neurons in mesoglea. Scale bars: a, g: 10 μ m; b, f: 30 μ m; c: 40 μ m; d, e: 50 μ m; h: 20 μ m; i: 15 μ m [Color figure can be viewed at wileyonlinelibrary.com]

identified numerous receptors on the surface of the body, presumably mechanoreceptors, that contained a single large cilium up to 10 μ m in length (Figure 15f and 21a,b, and 22). Contrary to *Euplokamis* receptors, this stereocilium was labeled by phalloidin only—similarly to receptors type 1 that we described in *P. bachei* and *B. abyssicola* (Norekian &

Moroz, 2019a, 2019b). Lobata ctenophores, such as *Mnemiopsis* and *Bolinopsis*, had a very high density of these single cilium receptors on the inside surface of their feeding lobes (Figure 16d,g). In all studied species, we also identified receptors of type 2—with multiple stereocilia labeled by phalloidin (Figure 15f and 22). It appeared that density of receptors,

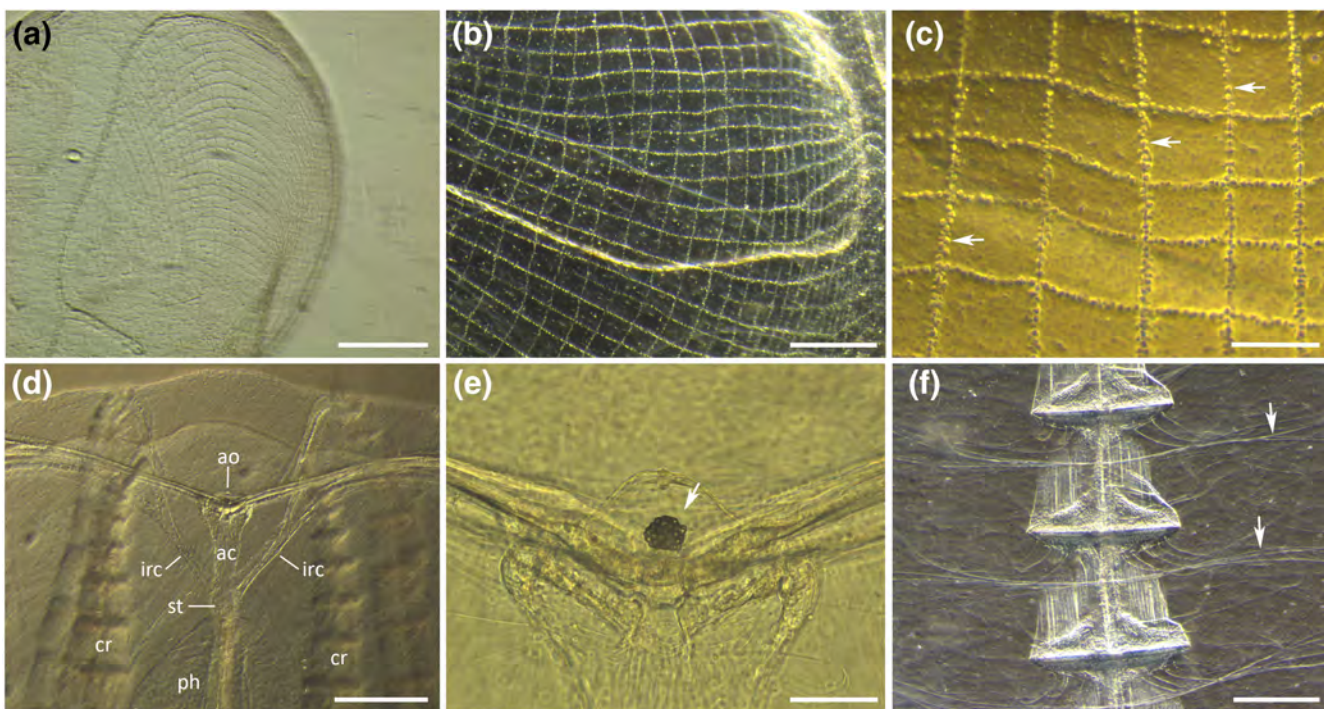


FIGURE 17 Light microscopy of adult *Mnemiopsis*. ac, Inside surface of the feeding lobes is covered with the rectangular network, which includes muscle fibers and neural mesh of processes and cell bodies (arrows indicate some). d, e, Aboral organ at different magnifications. Statolith is indicated by the arrow. f, Long muscle fibers attached to the comb rows (arrows show some). ao, aboral organ; ac, aboral canal; cr, comb row; irc, interradial canal; ph, pharynx; st, stomach. Scale bars: a: 700 μ m; b, d, f: 500 μ m; c: 200 μ m; e: 100 μ m [Color figure can be viewed at wileyonlinelibrary.com]

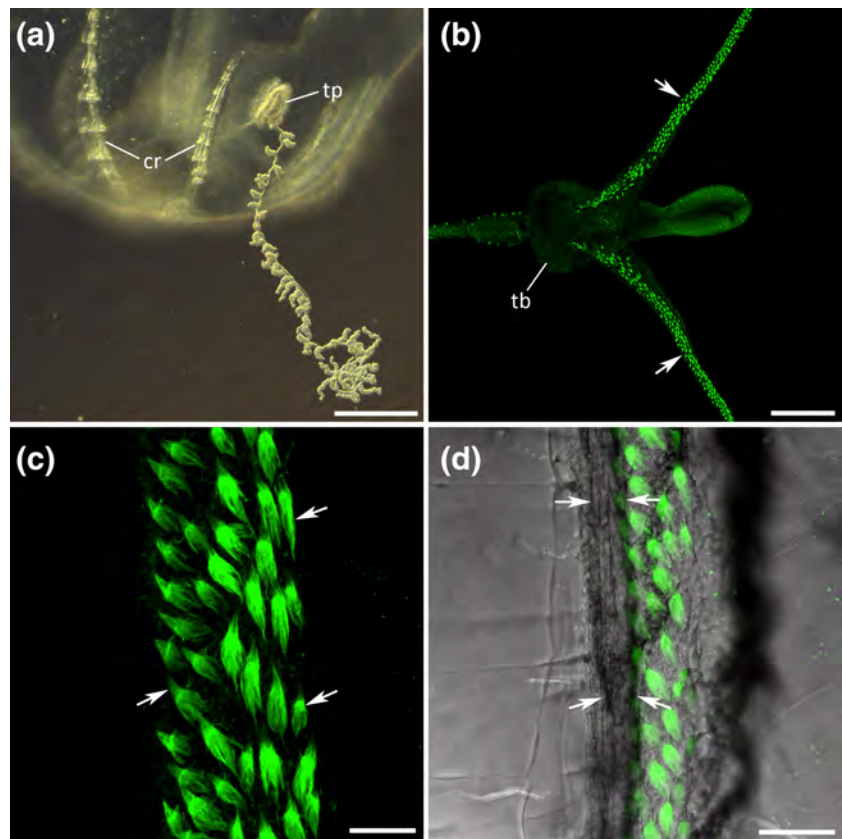


FIGURE 18 Tentacles and tentacular ciliated grooves in adult *Mnemiopsis* (tubulin antibody labeling is green). a, Tentacle in juvenile *Mnemiopsis* withdraws inside the tentacle pocket (tp) or sheath. b, In adult animals, tentacle sheaths disappear. Instead, on both sides of the tentacle base (tb), ciliated auricular grooves (arrows) are formed. c, Each auricular groove is covered by clusters of cilia (arrows), which are labeled by tubulin antibody. d, Tentacle (outlined by arrows) inside the ciliated groove (differential interference contrast). cr, comb row; tb, tentacle bulb; tp, tentacle pocket. Scale bars: A: 1 mm; b: 400 μ m; c: 40 μ m; d: 50 μ m [Color figure can be viewed at wileyonlinelibrary.com]

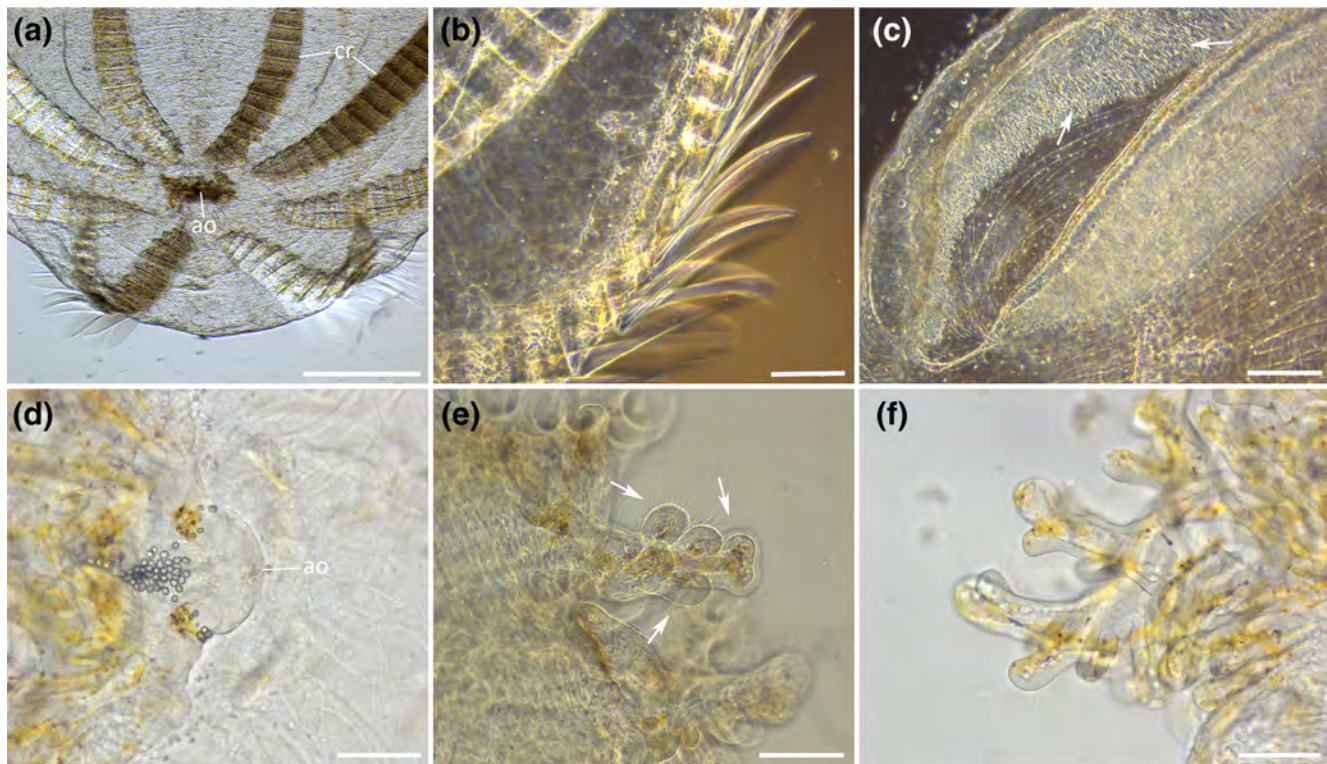


FIGURE 19 Light microscopy of adult *Beroe ovata*. a, The aboral end of the animal (ao, aboral organ; cr, comb rows). b, Long swim cilia in the comb row. c, Wide partially opened mouth with teeth-like feeding macrocilia indicated by arrows. d, Aboral organ (ao). e, f, Unique for *Beroe* large protruding lobes of the polar fields. Arrows show the long cilia covering the lobes. Scale bars: a: 1 mm; b, c: 200 μ m; d, e, f: 100 μ m [Color figure can be viewed at wileyonlinelibrary.com]

especially of the first type, with a single stiff cilium, was higher in *Bolinopsis* and *Mnemiopsis* than in *Dryodora*.

The muscle system in different species also had a similar basic structure but with some significant variations based on animals' morphology and behavior. There was a layer of parietal muscles representing a loose rectangular network of individual fibers below the epithelial or pharynx endothelial layers (*Beroe* in Figure 21D; *Mnemiopsis* in Figure 23a). Radial muscle fibers were crossing the mesogleal region from pharynx to the outer body wall (*Mnemiopsis*—see Figure 23b). In a *Mertensiidae* species, we identified the same type of radial muscles as in *Euplokamis*, which connect the aboral canal with the outer wall (Figure 24).

However, in *Lobata*, the long muscle fibers that are attached to the comb rows and then extend deep into the mesogleal region look differently (Figure 23c) compared to other studied ctenophores. In *Mnemiopsis* and *Bolinopsis*, these muscles are grouped into bundles, which are “squeezed” between the individual ctenes (Figures 17f and 23c). But in all other species, they are evenly distributed throughout the entire length of the comb row.

4 | DISCUSSION

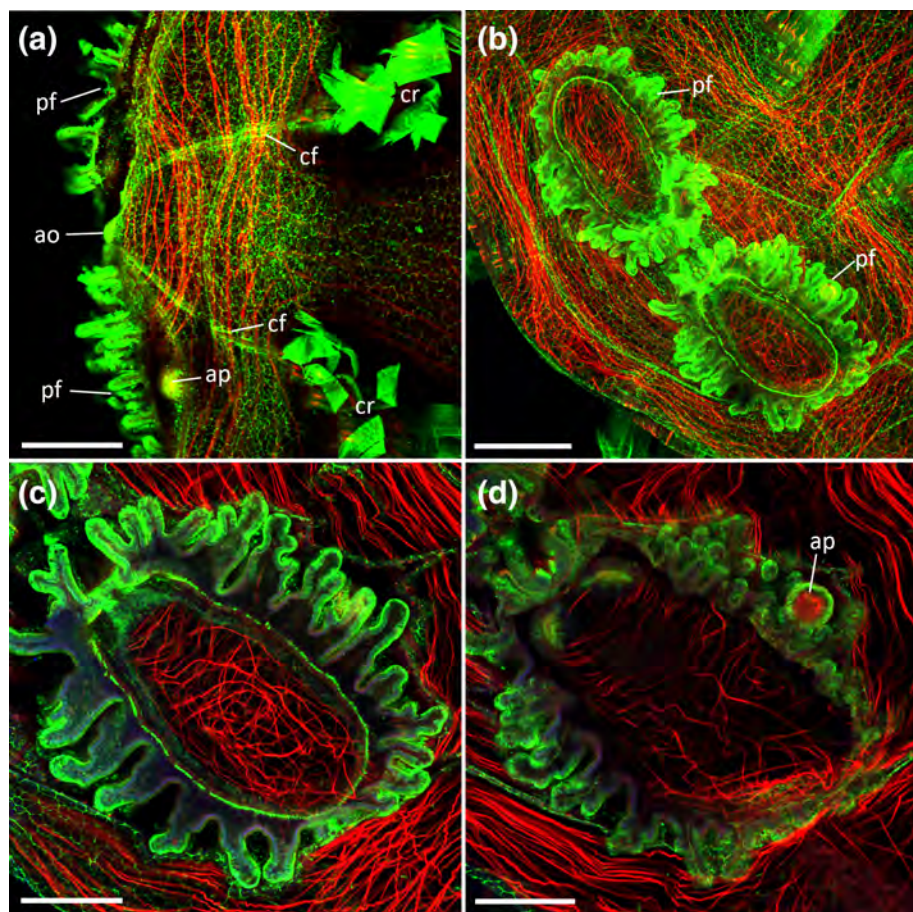
In summary, the basic ultrastructural and anatomical organization of the ctenophore neural system is similar among all studied species (Hernandez-Nicase, 1991; Jager et al., 2011; Moroz, 2015;

Norekian & Moroz, 2019a, 2019b). Two major subsystems were revealed: the subepithelial neural net and mesogleal network as well as a comparable subset of neuronal and receptor types (Norekian & Moroz, 2019a, 2019b). It implies substantial evolutionary conservative mechanisms underlying the maintenance of such neuronal architecture across the entire ctenophore lineage over at least 350 million years (Whelan et al., 2017).

On the other hand, within the same neuronal overall architecture, we observed some differences, which might reflect quite distinct behaviors across species. For example, *Euplokamis* is much more active and probably the fastest among known ctenophores with its rapid escape swimming patterns. Although the overall comb rows structure is very conservative and similar between *Euplokamis* and *Pleurobrachia*, swim cilia are significantly longer in *Euplokamis*. The development of longer cilia is an adaptive mechanism to increase the speed of swimming in general and escape swimming in particular. Even though the absolute length of the swim cilia is greater in a large *Beroe* specimen, when presented as a ratio of body size, they are much greater in smaller *Euplokamis*, and probably the greatest among ctenophores.

The most striking adaptation in *Euplokamis* was observed at the level of neuronal organization. Fast escape responses in many animals are often associated with the development of a system of large axons. Following the same evolutionary trend, the *Euplokamis* lineage

FIGURE 20 The aboral organ in *Beroe ovata*. Phalloidin staining is red, while tubulin IR is green. a, Side view of the aboral organ area. b, Horizontal view of the aboral organ and polar fields. Note the large lobes are forming a crown around each polar field, unique to *Beroe* species. c, d, Different optical sections through the polar fields showing the muscle fibers inside the polar field (c) and anal pore next to the polar field (d). *ap*, anal pore; *ao*, aboral organ; *cf*, ciliated furrows; *cr*, comb row; *pf*, polar fields. Scale bars: a, b: 300 μ m; c, d: 150 μ m [Color figure can be viewed at wileyonlinelibrary.com]



convergently evolved the system of “giant axons” (Mackie et al., 1992). Such a unique feature dramatically helps to hasten the propagation of signals and accomplish the effective global coordination of cilia beating in all rows. The comb row nerve runs along each swim row and connects them to the aboral organ, therefore, forming a basis for a very fast propagation and coordination of electrical signals.

Fast and low latency escape response requires a simultaneous beating of all swim cilia from different comb rows. The neural loop of the comb row nerves connects the “sister” nerves and consequently might provide a more direct level of coordination between neighboring comb rows; it could even bypass the control from the aboral organ.

As in other ctenophores, *Euplokamis* has a subepithelial neural network, which covers the entire surface area of the body with similar size polygonal units. This species also has the same types of mesogleal neurons as in other species: bipolar cells, multipolar cells, and cells giving rise to long thin processes crossing the mesoglea.

Finally, in *Euplokamis*, we have identified the same three types of surface receptors associated with the diffused neural network as in *Pleurobrachia* and *Beroe* (Norekian & Moroz, 2019a, 2019b). For comparative analysis, the most interesting was the type of receptors with a long and thick single cilium, which probably function as mechanoreceptors. These receptors, although longer in *Beroe*, were, as a ratio of body size, more prominent in *Euplokamis* than in any other

ctenophore. It is interesting that in *Euplokamis*, they were labeled by tubulin antibody whereas in *Pleurobrachia*, and *Beroe*, they were labeled by phalloidin only (Norekian & Moroz, 2019a, 2019b). This observation implies molecular differences between these probably homologous sensory structures. They were the most numerous receptors in *Euplokamis*, and if, as we suggest, they are fast-responding mechanoreceptors, it would account for the animal's high sensitivity to mechanical stimulation. In contrast, receptors with multiple cilia were the most abundant in *Beroe* (Norekian & Moroz, 2019a).

Euplokamis and *Pleurobrachia* are both ctenophores with a similar cydippid body plan (Figure 1), including a pair of long tentacles that they use to catch the prey. But, there are two striking differences between these two species in the structure of the muscle system. The body shape in *Pleurobrachia* is supported by rigid hydrokeleton, which significantly limits the body movements and does not require strong muscular support. As a result, there are relatively few muscle fibers, and they are thin and possibly less powerful than in other ctenophores (except the flat muscles connected to the comb rows). In *Euplokamis*, however, we have found numerous (‘powerful’) bundles of radial muscles crossing the mesogleal region and connecting the aboral canal with the outer surface body wall. We speculate that these muscles might mediate the body contractions associated with the startle response in *Euplokamis* as well as other behaviors.

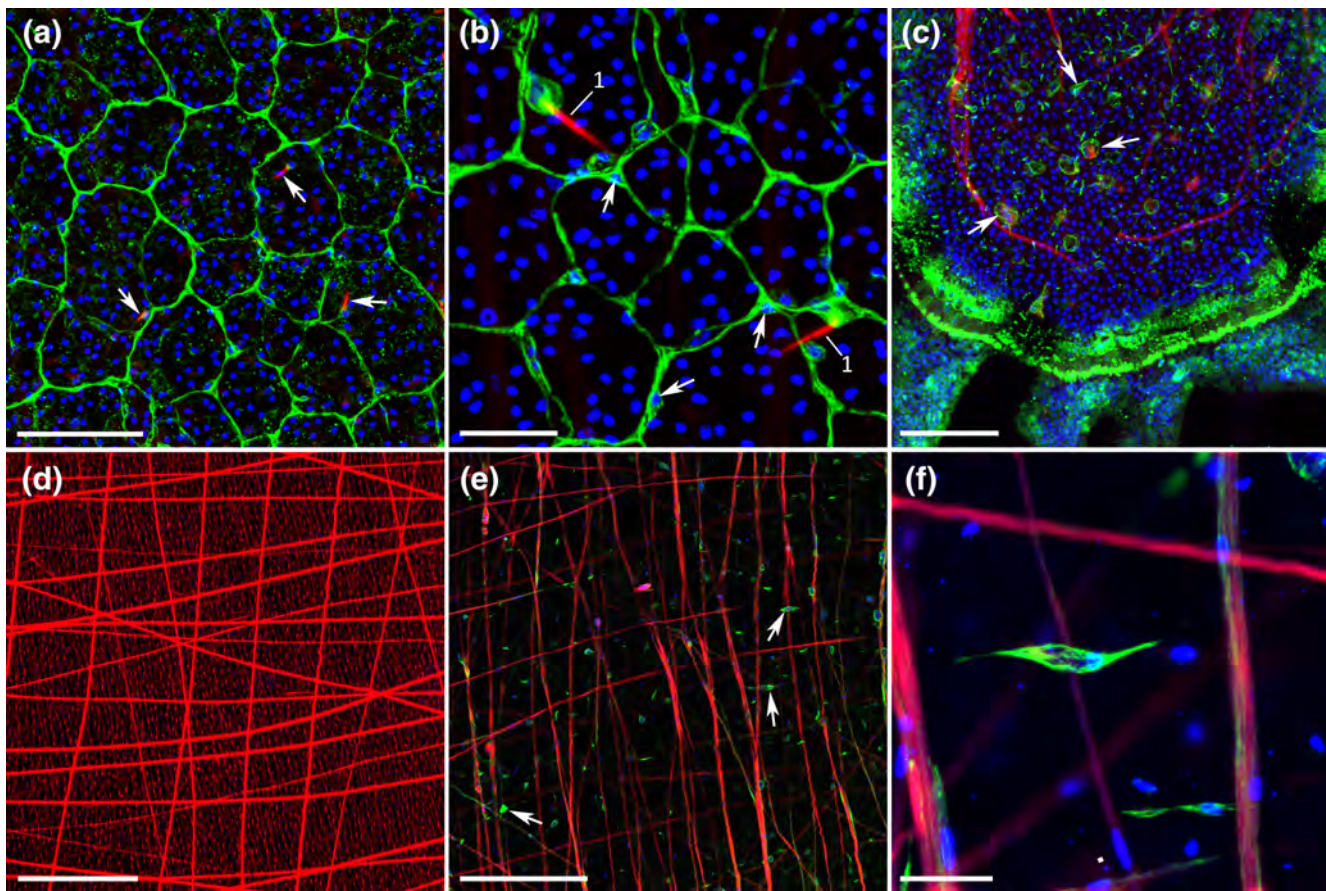


FIGURE 21 The neural system of *Beroe ovata*. Tubulin IR is shown in green, phalloidin staining is red, while nuclear DAPI staining is blue. a, Subepithelial neural network. Arrows show some of the single-cilium mechanoreceptors on the surface of the body. b, Two putative mechanoreceptors at higher magnification (receptor type 1). Note also numerous nuclei in the strands of the network (arrows). c, Tubulin-ir cells inside the polar fields. d, Parietal muscle fibers are criss-crossing the wall of the pharynx. e, Muscle fibers and neurons (arrows show some) in the mesoglea. f, Large bipolar neuron in the mesoglea at high magnification. Scale bars: a, c: 50 μ m; b, f: 20 μ m; d, e: 200 μ m [Color figure can be viewed at wileyonlinelibrary.com]

The second major difference between *Euplokamis* and other ctenophores is the presence of striated muscles in the tentilla (in addition to conventional smooth muscles). These muscles are instrumental in a fast discharge (uncoiling) of the tentilla during prey capture (Mackie et al., 1988; Mackie et al., 1992). During the prey capture, *Euplokamis* is significantly faster and more active than *Pleurobrachia* and, therefore, have developed specialized innovations to support that behavior. Very fast and complex behavioral responses of tentacles during feeding in *Euplokamis* are also reflected in more complex innervation of the tentilla. We identified several rows of large axons in *Euplokamis* tentilla, which were not seen in other cydippids, along the rows of "boxes" that provide mechanical support for tentilla. They presumably provide the neural basis for extremely fast tentilla reactions during feeding.

A very interesting deviation from the conserved structure of the subepithelial neural network in ctenophores was observed in two species, *Mnemiopsis* and *Bolinopsis*, which belong to the order Lobata. The lobates have a pair of broad feeding lobes, which

represent muscular scoop-like extensions of the main body on either side of the mouth. These lobes are very sensitive to mechanical stimulation and contain numerous muscles. As a result, these lobes can constantly change their shape during feeding. Most of the sensitivity is expected on the inner surface of the lobes, which encounter the food. Correspondingly, we have found a very high density of single cilium mechanoreceptors on the inner surface of feeding lobes. This inner surface area also had the subepithelial neural network, which was quite different from the rest of the integument in *Bolinopsis* and *Mnemiopsis*, as well as the other studied ctenophores. First, the network had only large uniformed rectangular units, and not usual polygonal units of different sizes and shapes. The strands of the neural network ran parallel to the muscle filaments that had the same orientation in the inner wall of feeding lobes. And importantly, the strands of the mesh were covered with numerous and large round-shaped cell bodies (presumably neural-like type), which looked like grapes on the vine. Such a large number of neuroid cells and the spatial orientation of the network strands along the

FIGURE 22 Surface receptors in *Dryodora* (phalloidin is red, tubulin antibody is green, while DAPI is blue). a, b, Receptors of the first type (1) with a single stereocilium and receptors of the second type (2) with multiple stereocilia. c, d, Higher magnification of two receptor types. Scale bars: a, b: 30 μ m; c, d: 10 μ m [Color figure can be viewed at wileyonlinelibrary.com]

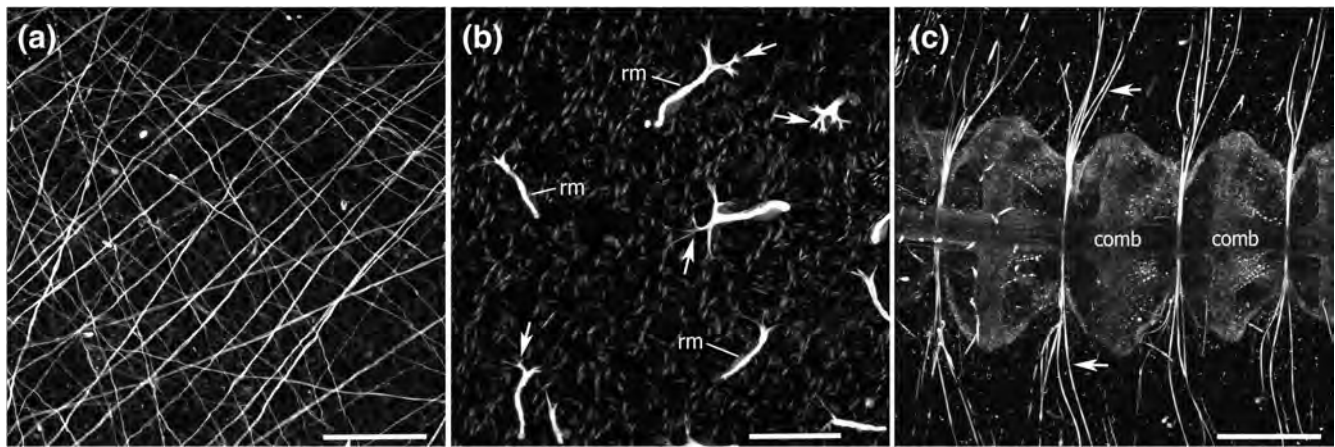
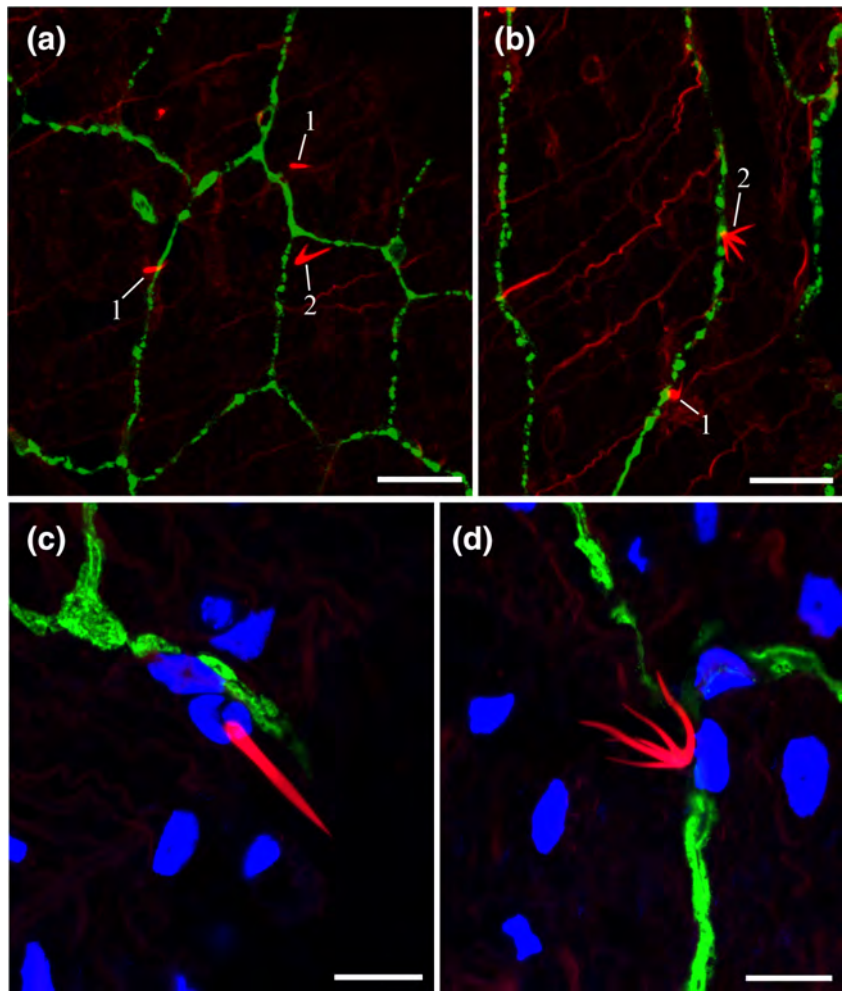


FIGURE 23 Muscles labeled by phalloidin in *Mnemiopsis*. a, Parietal muscle fibers in the outside wall form a loose rectangular network. b, Radial muscles (rm) cross the mesoglea and connect the pharynx wall with the outer body wall. Arrows show extensive branching of radial muscles at the attachment with pharynx wall. c, Long muscle fibers (arrows) attached to the comb rows and extended deep into the mesoglea. Scale bars: a: 200 μ m, b: 100 μ m, c: 250 μ m

muscle fibers presumably reflects both the high sensitivity and active shape changing of the feeding lobes in the Lobata ctenophores. However, the physiological data about these grape-like cells are lacking, and their putative neural/secretory/signaling nature, as well

as the functional network organization, within the ctenophore feeding circuits should be a subject of future investigations.

In conclusion, although the *Euplokamis* represents one of the most basal branches of ctenophores lineages, its neuromuscular

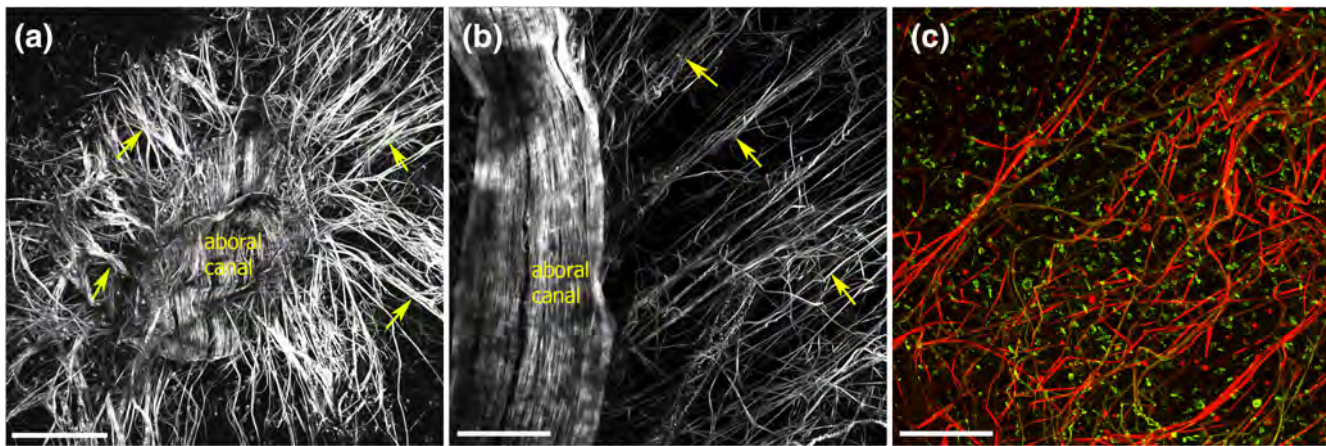


FIGURE 24 The muscular system of *Mertensiidae* sp. a, b, Numerous radial muscles (arrows) cross the mesoglea and connect the aboral canal at the center of the body with the outside body wall—phalloidin labeling. c, Mesogleal region is filled with muscle fibers (stained in red by phalloidin) and neural cells (labeled by tubulin antibody in green). Scale bars: a, b, c: 200 μ m [Color figure can be viewed at wileyonlinelibrary.com]

organization is among the most complex with sophisticated innovations (striated muscles and giant axons), which convergently evolved in this group of animals, independently from analogous structures in bilaterians.

ACKNOWLEDGMENTS

We thank FHL for their excellent collection and microscope facilities. We also thank Drs. Claudia Mills for useful ctenophore discussions, Olga Krivenko and Maxim Kirin for help and collecting *Mnemiopsis* and *Beroe ovata*. This work was supported by the United States National Aeronautics and Space Administration (grant NASA-NNX13AJ31G), the National Science Foundation (grants 1146575, 1557923, 1548121 and 1645219), and Human Frontiers Research Program (LLM), as well as the Ministry of Education and Science of the Russian Federation grant 14.W03.31.0015 (TPN).

CONFLICT OF INTEREST

The authors declare no potential conflict of interest.

AUTHORS CONTRIBUTIONS

All authors had full access to all the data in the study and take responsibility for the integrity of the data and the accuracy of the data analysis. TPN and LLM share authorship equally. Research design: TPN, LLM. Acquisition of data: TPN, LLM. Analysis and interpretation of data: TPN, LLM. Drafting of the article: TPN, LLM. Funding: LLM.

DATA AVAILABILITY STATEMENT

The data that support the findings of this study are available from the corresponding author upon request.

ORCID

Tigran P. Norekian <https://orcid.org/0000-0002-7022-1381>

Leonid L. Moroz <https://orcid.org/0000-0002-1333-3176>

REFERENCES

Arcila, D., Ortí, G., Vari, R., Armbruster, J. W., Stiassny, M. L. J., Ko, K. D., ... Betancur, R. R. (2017). Genome-wide interrogation advances resolution of recalcitrant groups in the tree of life. *Nature Ecology & Evolution*, 1(2), 20.

Borowiec, M. L., Lee, E. K., Chiu, J. C., & Plachetzki, D. C. (2015). Extracting phylogenetic signal and accounting for bias in whole-genome data sets supports the Ctenophora as sister to remaining Metazoa. *BMC Genomics*, 16, 987.

Brusca, R. C., & Brusca, G. J. (2003). *Invertebrates* (p. 936). Sunderland, MA: Sinauer Associates, Inc.

Chun, C. (1880). *Die Ctenophoren des Golfs von Neapel, und der angrenzenden Meeres-Abschnitte* (p. 1880). Leipzig, Germany: W. Engelmann.

Dunlap, P. H. (1974). Ctenophore. In A. C. Giese & J. S. Pearse (Eds.), *Reproduction of marine invertebrates Vol 1, acelomate and pseudocoelomate metazoans* (pp. 201–265). New York: Academic Press.

Dunn, C. W. (2017). Ctenophore trees. *Nature Ecology & Evolution*, 1(11), 1600–1601.

Dunn, C. W., Hejnol, A., Matus, D. Q., Pang, K., Browne, W. E., Smith, S. A., ... Giribet, G. (2008). Broad phylogenomic sampling improves resolution of the animal tree of life. *Nature*, 452(7188), 745–749.

Dunn, C. W., Leys, S. P., & Haddock, S. H. (2015). The hidden biology of sponges and ctenophores. *Trends in Ecology & Evolution*, 30(5), 282–291.

Granhaug, L., Majaneva, S., & Møller, L. F. (2012). First recording of the ctenophore *Euplokamis dunlapae* (Ctenophora, Cydippida) in Swedish waters. *Aquatic Invasions*, 7(4), 455–463.

Halanych, K. M. (2015). The ctenophore lineage is older than sponges? That cannot be right! Or can it? *The Journal of Experimental Biology*, 218(4), 592–597.

Hernandez-Nicase, M.-L. (1991). Ctenophora. In F. W. Harrison & W. J. A. FW (Eds.), *Microscopic anatomy of invertebrates: Placozoa, Porifera, Cnidaria, and Ctenophora* (Vol. 2, pp. 359–418). New York: Wiley.

Jager, M., Chiori, R., Alie, A., Dayraud, C., Queinnec, E., & Manuel, M. (2011). New insights on ctenophore neural anatomy:

Immunofluorescence study in *Pleurobrachia pileus* (Muller, 1776). *Journal of Experimental Zoology. Part B, Molecular and Developmental Evolution*, 316B(3), 171–187.

Jager, M., Dayraud, C., Mialot, A., Queinnec, E., le Guyader, H., & Manuel, M. (2013). Evidence for involvement of Wnt signalling in body polarities, cell proliferation, and the neuro-sensory system in an adult ctenophore. *PLoS One*, 8(12), e84363.

Johansson, M. L., Shiganova, T. A., Ringvold, H., Stupnikova, A. N., Heath, D. D., & MacIsaac, H. J. (2018). Molecular insights into the ctenophore genus *Beroe* in Europe: New species, spreading invaders. *The Journal of Heredity*, 109(5), 520–529.

Kozloff, E. N. (1990). *Invertebrates* (p. 866). Philadelphia, PA: Sounders College Publishing.

Mackie, G. O., Mills, C. E., & Singla, C. L. (1988). Structure and function of the prehensile tentilla of *Euplokamis* (Ctenophora, Cydippida). *Zoomorphology*, 107, 319–337.

Mackie, G. O., Mills, C. E., & Singla, C. L. (1992). Giant axons and escape swimming in *Euplokamis dunlapae* (Ctenophora: Cydippida). *The Biological Bulletin*, 182(2), 248–256.

Mills, C. E. (1987). Revised classification of the genus *Euplokamis* Chun, 1880 (Ctenophora: Cydippida: Euplokamidae. Fam.) with a description of the new species *Euplokamis dunlapae*. *Canadian Journal of Zoology*, 65, 2661–2668.

Moroz, L. L. (2014). The genealogy of genealogy of neurons. *Communicative & Integrative Biology*, 7(6), e993269.

Moroz, L. L. (2015). Convergent evolution of neural systems in ctenophores. *The Journal of Experimental Biology*, 218(4), 598–611.

Moroz, L. L. (2018). NeuroSystematics and periodic system of neurons: Model vs reference species at single-cell resolution. *ACS Chemical Neuroscience*, 9(8), 1884–1903.

Moroz, L. L., Kocot, K. M., Citarella, M. R., Dosung, S., Norekian, T. P., Povolotskaya, I. S., ... Kohn, A. B. (2014). The ctenophore genome and the evolutionary origins of neural systems. *Nature*, 510(7503), 109–114.

Moroz, L. L., & Kohn, A. B. (2015). Unbiased view of synaptic and neuronal gene complement in ctenophores: Are there pan-neuronal and pan-synaptic genes across Metazoa? *Integrative and Comparative Biology*, 55(6), 1028–1049.

Moroz, L. L., & Kohn, A. B. (2016). Independent origins of neurons and synapses: Insights from ctenophores. *Philosophical Transactions of the Royal Society of London. Series B, Biological Sciences*, 371(1685), 20150041.

Norekian, T. P., & Moroz, L. L. (2016). Development of neuromuscular organization in the ctenophore *Pleurobrachia bachei*. *The Journal of Comparative Neurology*, 524(1), 136–151.

Norekian, T. P., & Moroz, L. L. (2019a). Neural system and receptor diversity in the ctenophore *Beroe abyssicola*. *The Journal of Comparative Neurology*, 527, 1986–2008.

Norekian, T. P., & Moroz, L. L. (2019b). Neuromuscular organization of the ctenophore *Pleurobrachia bachei*. *The Journal of Comparative Neurology*, 527(2), 406–436.

Sebe-Pedros, A., Chomsky, E., Pang, K., Lara-Astiaso, D., Gaiti, F., Mukamel, Z., ... Tanay, A. (2018). Early metazoan cell type diversity and the evolution of multicellular gene regulation. *Nat Ecol Evol*, 2(7), 1176–1188.

Shen, X. X., Hittinger, C. T., & Rokas, A. (2017). Contentious relationships in phylogenomic studies can be driven by a handful of genes. *Nature Ecology & Evolution*, 1(5), 126.

Simion, P., Philippe, H., Baurain, D., Jager, M., Richter, D. J., Di Franco, A., ... Manuel, M. (2017). A large and consistent phylogenomic dataset supports sponges as the sister group to all other animals. *Current Biology*, 27(7), 958–967.

Steinmetz, P. R., Kraus, J. E., Larroux, C., Hammel, J. U., Amon-Hassenzahl, A., Houlston, E., ... Technau, U. (2012). Independent evolution of striated muscles in cnidarians and bilaterians. *Nature*, 487(7406), 231–234.

Striedter, G. F., Belgard, T. G., Chen, C. C., Davis, F. P., Finlay, B. L., Gunturkun, O., ... Wilczynski, W. (2014). NSF workshop report: Discovering general principles of nervous system organization by comparing brain maps across species. *The Journal of Comparative Neurology*, 522(7), 1445–1453.

Tamm, S. L. (1982). *Ctenophora. Electrical conduction and behavior in "simple" invertebrates* (pp. 266–358). Oxford: Clarendon Press.

Tamm, S. L. (2014). Cilia and the life of ctenophores. *Invertebrate Biology*, 133(1), 1–46.

Tamm, S. L., & Tamm, S. (1987). Massive actin bundle couples macrocilia to muscles in the ctenophore *Beroe*. *Cell Motility and the Cytoskeleton*, 7(2), 116–128.

Telford, M. J., Moroz, L. L., & Halanych, K. M. (2016). Evolution: A sisterly dispute. *Nature*, 529(7586), 286–287.

Wehland, J., & Willingham, M. C. (1983). A rat monoclonal antibody reacting specifically with the tyrosylated form of alpha-tubulin. II. Effects on cell movement, organization of microtubules, and intermediate filaments, and arrangement of golgi elements. *The Journal of Cell Biology*, 97(5), 1476–1490.

Wehland, J., Willingham, M. C., & Sandoval, I. V. (1983). A rat monoclonal antibody reacting specifically with the tyrosylated form of alpha-tubulin. I. Biochemical characterization, effects on microtubule polymerization in vitro, and microtubule polymerization and organization in vivo. *The Journal of Cell Biology*, 97(5), 1467–1475.

Whelan, N. V., Kocot, K. M., Moroz, L. L., & Halanych, K. M. (2015). Error, signal, and the placement of Ctenophora sister to all other animals. *Proceedings of the National Academy of Sciences of the United States of America*, 112(18), 5773–5778.

Whelan, N. V., Kocot, K. M., Moroz, T. P., Mukherjee, K., Williams, P., Paulay, G., ... Halanych, K. M. (2017). Ctenophore relationships and their placement as the sister group to all other animals. *Nature Ecology & Evolution*, 1(11), 1737–1746.

Wulf, E., Deboren, A., Bautz, F. A., Faulstich, H., & Wieland, T. (1979). Fluorescent phallotoxin, a tool for the visualization of cellular Actin. *Proceedings of the National Academy of Sciences of the United States of America*, 76(9), 4498–4502.

SUPPORTING INFORMATION

Additional supporting information may be found online in the Supporting Information section at the end of this article.

How to cite this article: Norekian TP, Moroz LL. Comparative neuroanatomy of ctenophores: Neural and muscular systems in *Euplokamis dunlapae* and related species. *J Comp Neurol*. 2019;1–21. <https://doi.org/10.1002/cne.24770>